Design of a Bi-Directional Fly-back DC/DC Converter

For a stand-alone solar-powered eBike charging station

Bas van der Werk, Thomas Gerrits & George Koolman

Bachelor Thesis

TU Delft Delft University of Technology

Design of a Bi-Directional Flyback DC/DC Converter

For a stand-alone solar-powered eBike charging station

Bachelor Thesis

Group B2

George Koolman	4270975
Bas van der Werk	4346785
Thomas Gerrits	4355075

June, 2017

Faculty of Electrical Engineering, Mathematic and Computer Science (EEMCS)
Delft University of Technology


TU Delft
Delft
University of
Technology

Acknowledgements

We would first like to thank our supervisor dr. ir. P. J. van Duijsen for giving us an interesting and technically challenging BAP free elective and also for taking the time from his busy schedule to intensely help us understand the power concepts and challenges faced in DC/DC converters. It was surely helpful and motivated some of us to consider further pursuing a masters degree in power engineering.

Secondly, we would like to thank Joris Koeners, Harrie Olsthoorn, Chris Swanink, Bart Rodenburg and the Dream-hall for helping us get the needed equipment and location to successfully work on our BAP thesis.

Lastly, we would also like to thank Pavel Purgat for his expertise and advice during troubleshooting of our prototype and Martin Schumacher for being the administrative contact.

Executive Summary

This document is the bachelor graduation thesis of BAP Group B2. Together with BAP Group B1 the objective of this project was to create a control network and DC/DC converter implementation capable of fast, analog power management with active, remote-control and -interfacing of multiple converter's energy flows. The system will be designed to function in the solar-powered eBike charging station on the TU Delft campus.

This document specifically is concerned with the design, simulation and testing of the DC/DC converter. The thesis presents a bi-directional flyback DC/DC converter design and prototype with analog power management, universal control signals and high integration potential.

These aspects are accomplished by building upon the traditional flyback DC/DC converter design with respect to circuit topology, power-flow control, connectivity and accessibility. The difficult regulation and measurement of DC power flow has been reduced to a set of analog signals interpretable by any microcontroller, easing the integration of the converter into larger energy and control networks.

A working prototype is presented and the inner-workings of the electrical circuit are discussed and evaluated in detail. The converter is tested beyond the limit of the design requirements and the performance is documented. Provided are possible reasons for malfunctioning and guidelines for future improvements.

Table of Contents

Problem Description

1.1 Problem Scope

The current electrical power grids have seen a considerable increase in contributors and recipients in the form of off-shore wind-farms, enormous solar-fields, electric vehicle (EV) infrastructure and extensive consumer electronics, among others. The growth of these non-conventional power elements in the distribution chain conflict with the functionality of traditional electrical grids, designed in the 20th century. The traditional grids struggle with the energy surges and droughts produced by sustainable energy technologies such as solar and wind, and do not make use of the technologies available in the 21st century.

In new, state-of-the-art grids not only power, but also information is generated and exchanged in the infrastructure. This allows analysis of the power flow, and control and scheduling of the enclosed system. Energy demands can be adjusted to meet the available supplies, whereas in the current systems, demand control is severely lacking.

The purpose of this thesis is to design a robust bi-directional flyback DC/DC converter with fast, analog control and the potential of integration into a vast range of prospective electrical grids. In it's most simple form the converter needs to be able to charge Lithium-Ion batteries of electric bicycles and it will be designed as a key element of the solar-powered eBike charging station developed at the TU Delft faculty, EEMCS[19].

1.2 Technical Review

Energy flow Managing and controlling the flow of energy is an important aspect in current electrical grids. Small or large grids would benefit from integrated power management on an analog level. New DC-microgrids, like solar-powered green villages[2] or DC-fed automotive boardnets, are being designed to function completely free from any external energy source. These grids have a significant amount of varying supplies, loads and hybrid elements like batteries. They need to manage their energy flow and storage with complex algorithms in order to function efficiently and reliably.

Switch mode power supplies One possible way to do this is with the use of a flyback converter. The flyback converter that is proposed is a subcategory of the so called Switch Mode Power Supplies (SMPS). In its most basic form a switch mode power supply uses a switching component, an inductor and a rectifying diode to transfer DC or AC power to DC loads, while converting the electrical characteristics of the power flow. or transfer energy from the input to the output. Currently, SMPS are rapidly replacing linear regulated power supplies in most

modern electronic devices. They often show higher efficiency, better output voltage regulation and compacter size.

Linear power supplies basically consists of a dissipative series regulator and a transformer. Normally the transformer is a heavy 50/60 Hz transformer which increases the cost, size and weight. Efficiencies of a linear voltage regulator are quite low, often not higher then 60 percent. SMPS however, are able to function at frequencies that range from several hz to several hundred kHz. Especially when looking at frequencies of a few tens of kHz the SMPS shows great results, and efficiencies up 80 or 90 percent can be achieved. Switching at higher frequencies also reduces the size of filtering components and the transformer[3].

1.3 Design Requirements

The converter will be used in the solar-powered eBike charging station which determines a set of initial design guidelines. A couple of general design requirements(req) and wishes(wish) have been formulated to fulfill this intention, while also keeping the door open for future innovation and integration.

- The output power needs to be 110 Watts (req).
- The input voltage can vary between 36 and 48 volts (req).
- Add functionality at low input voltages ranging from 12V and up (wish).
- The required output power needs to be met at an output voltage of 48V (req).
- The flyback converter has a wide output voltage range that can vary between 12V and 48V (wish).
- The flyback converter needs to have fast, analog cycle-to-cycle current limiting (req).
- The switching frequency needs to be settable to a maximum of 125 kHz (wish).
- The flyback converter needs to operate in discontinuous current mode (wish).
- The flyback converter needs to be able of bi-directional energy conversion (wish).
- Low ripple on the output voltage line (wish).
- The flyback converter needs to be controlled by a simple microcontroller, while providing measurements of the DC power flow (req).
- The flyback converter needs to be applicable in a number of other circumstances, such as smart DC-grids (wish).
- The flyback converter needs to be a robust design to maximize lifetime (wish).

Design Description

2.1 Overview

The bi-directional flyback converter proposed is part of a larger network of multiple DC/DC power converters and control circuitry shown in figure 2-1. This system is able to effectively manage, control and display the energy flow wherever the power converters are implemented. The conversion of the DC power happens on-board by the use of the flyback SMPS circuit topology, controlled by digital commands received from a slave. The master and slave receive relevant information about the power flow from the converter and determine a course of action. All this information is sent to a server where real-time status can be observed and commands can be sent back to the converter from any device connected to the internet.

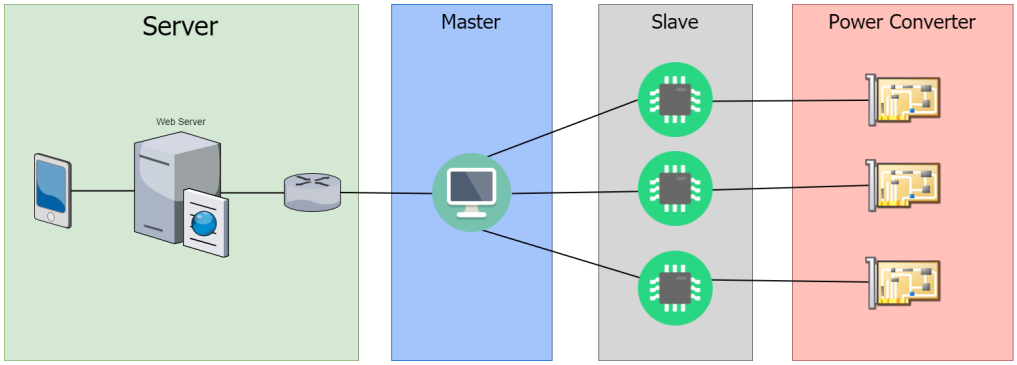

Figure 2-1: Simplified diagram of the complete standalone charging system

Our design focuses explicitly on the power converter block and the implementation of the control signals and measurements to and from the slave. The power converters in this block are all bi-directional flyback converters.

These converters are designed keeping all requirements of section 1.3 in mind, while also trying to fulfill as much of the additional wishes as possible.

Flyback Topology

The flyback topology is derived from the buck-boost topology. This is achieved by replacing the inductor in a buck-boost converter with a coupled inductor, such as gapped core transformers [21]. The characteristics of the transformer enables the use of less components, while still retaining the same functionalities. Making the flyback a simpler and cheaper option.

In its simplest form the flyback consist of a switch on the primary side of the transformer and a diode with output capacitor on the secondary side. Bi-directionality is achieved by mirroring the components on both sides as shown in figure 2-2.

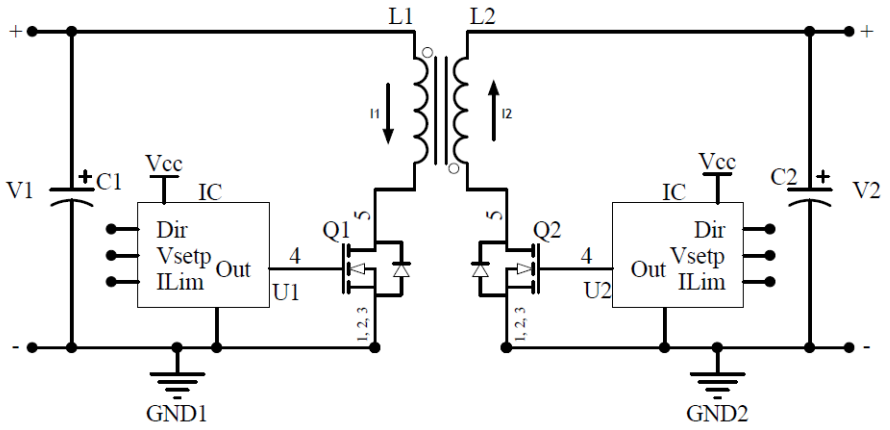

Figure 2-2: Simplified schematic of a bi-directional flyback converter

For the sake of simplicity the flyback topology will be explained with a one directional flyback. The energy transfer is described in two states, the ON and OFF state.

ON state In this state the MOSFET Q1 is turned on, meaning it will conduct and Q2 is turned off. The energy from the input is stored inside the transformer as magnetizing inductance. The output diode (internal MOSFET body diode Q2) is off (reverse biased) and energy is supplied to the load from the output capacitors [12].

OFF state Here MOSFET Q2 is turned off, the energy inside the primary side transfers to the secondary inductor, the voltage across the secondary inductor reverses and the internal MOSFET body diode Q2 turns on (forward bias). The stored energy is then supplied to the output capacitor and load [12].

The flyback converter can operate in two modes, discontinuous current mode (DCM) and continuous current mode (CCM). In DCM the current in the secondary inductor is fully delivered to the load before the next switching cycle. For our transformer design, this requires the duty cycle (D) to be under 50% (see figure 2-3 and section 2.2.1). In CCM on the other hand the next switching cycle begins while the secondary inductor still has current running through it [12]. For our application DCM is wishful.

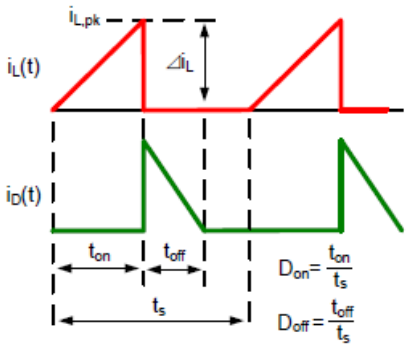

Figure 2-3: Currents during DCM operation

The advantages of DCM are:

- Higher efficiency.
- Faster transient response.
- Low primary inductance, thus making the transformer smaller [22].

However there are some drawbacks. DCM produces parasitics that cause higher peak currents which results in higher peak voltages over the MOSFET that can cause failures[21]. For this reason extra switching circuitry has been added to promote robustness of our flyback converter.

Converter Power management

Controlling the energy flow, there are PWM (Pulse Width Modulation) control IC's on either side, driving the MOSFETs. These produce the appropriate duty cycle to match the voltage set point (*Vsetp*), current limit (*Ilim*) and energy directon (*DIR*), received from the microcontroller.

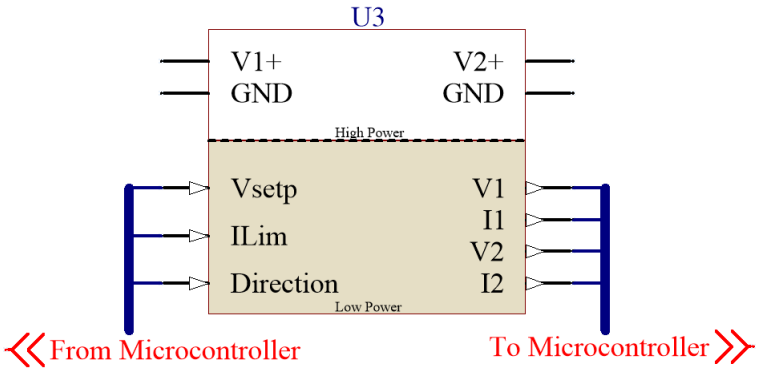

Figure 2-4: Control and measurement connections to the converter

Furthermore, the PWM controller itself is controlled via multiple subsystems. These subsystems consist of a Measurement Bridge, Digital to Analog Converters (DAC) and a Direction Comparator, and function as the translational step between the converter and the microcontroller. The measurement bridge does four measurements, the current and voltage of both the primary and the secondary side. These measurement signals are sent to the microcontroller. Using these measurements the microcontroller determines a course of action depending on implemented algorithms. The microcontroller initially sends two PWM signals back to the converter, *Vsetp* and *ILim*. These digital signals are received by the DAC and converted to an analog signal. The *Vsetp* signal 'sets' the output voltage and *ILim* limits the suppliable current. A third signal is sent from the microcontroller to determine the direction of energy flow through the flyback. Either from left to right or from right to left (see Figures 2-4 and 2-5).

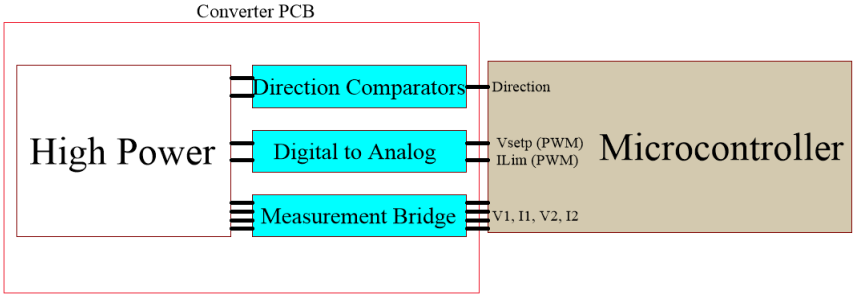

Figure 2-5: PCB signal conversion subsystems

2.2 Components

To obtain a properly functioning flyback converter it is essential to obtain components that work accurately and effectively. Especially the choices regarding the switching component, PWM controller and the transformer are crucial. For each of these component design parameters need to be established. This section gives an overview of the considerations made concerning these three components.

2.2.1 Transformer

In flyback converters, the transformer is a crucial component that needs to be carefully designed. The transformer needs to combine the functions of power transfer, energy storage, and galvanic isolation[12]. Many facets come into play when designing the coupled inductor. For macro-circuit design and operation, the turn ratio $\left(\frac{N_p}{N_s}\right)$ and magnetic core saturation (B_{sat}) are the most important factors. These aspects determine the input and output voltage and current characteristics of the overall circuit, as well as frequency limitations and ripple current[8].
A variety of other parameters are inherent to coupled inductors that influence the efficiency, stability and complexity. These include, but are not limited to; the primary and secondary coil inductance and turns, the parasitic inductance, the resistive winding and magnetic core losses, the core shape and air-gap. These parameters are a subject of initial design and have considerable importance, as they are a key factor in the overall performance and lifetime of the converter. This section gives insight in the design of a transformer[11].

Requirements

Besides the general requirements stated in section 1.3 there are a couple of requirements and wishes established specifically for the transformer.

- The transformer winding ratio is 1:1 in order to keep the currents on both primary and secondary side the same (wish).
- Leakage inductance needs to be as low as possible in order to prevent high over-voltage spikes, ringing and losses (wish).
- The maximal flux density is set to 300 mT. The flux density determines how much energy can be moved through a transformer. High flux density means more power can be moved through the transformer, however when the value is too high, power losses will rise drastically. 300 mT is often used as a rule of thumb[5] (req).
- The inductance value needs to be chosen as big as possible in order to minimize peak currents (wish).
- The core needs to be chosen as small as possible in order to have as few losses as possible (wish).
- The calculated number of turns necessary needs to fit on the coil former (req).
- The air gap should be as wide as possible in order to increase the inductance factor thus minimizing the number of layers and core size needed (wish).

Design

The design process of a transformer can be subdivided into several steps. The first step that needs to be made is picking a core type and size. Important requirements that need to be taken into account when looking at the core size are the flux density and the maximum output power. These will give a rough estimation on the type and size, however this does not mean that the originally chosen core is the correct one, since there is a possibility that a requirement will not be met and a different core needs to be chosen.
There is a wide variety of cores ranging from the magnetically superior POT cores to the more cheaper E and EE cores[9]. Since the E and EE cores offer the lowest cost with respect to other core types the focus will initially be on these type of cores.
The size of the core is based on an estimation of the amount of turns and output power. Furthermore, it is better to pick a bigger gap before picking a bigger core size. A smaller core has less heat radiation, lower losses and lower parasitic capacitances[10].

Next step is to calculate the number of turns. The following formula applies for the flux density,

$$B = \frac{A_L \cdot n \cdot I_{p,peak}}{A_{core}} \tag{2-1}$$

with,

- n, the number of turns.
- $I_{p,peak}$(A), the peak current at the primary side of the transformer.
- A_L(H), the inductance factor.
- B(T), the flux density.
- $A_{core}(m^2)$, the core area.

Rewriting this to the number of turns results in,

$$n = \frac{B \cdot A_{core}}{A_L \cdot I_{p,peak}} \tag{2-2}$$

The peak current of formula 2-2 is still unknown, which means that other parameters need to be looked into first before making an assumption on the number of turns.
For the output power the following formula applies,

$$P_{out} = 0.5 \cdot L_p \cdot I_{p,peak}^2 \cdot f \tag{2-3}$$

with:

- P_{out}(W), the output power.
- L_p(H), the primary inductance.
- f(Hz), the frequency.

Keeping in mind the required output power of 110 W, the peak current can be determined. Rewriting formula 2-3 to the peak current results in,

$$I_{p,peak} = \sqrt{\frac{2 \cdot P_{out}}{L_p \cdot f}} \tag{2-4}$$

This results in another unknown parameter, the primary inductance. The primary inductance is related to the peak current via the following equation,

$$I_{p,peak} \leq \frac{V_B \cdot D \cdot T}{L_p} \tag{2-5}$$

with,

- D, the duty cycle.
- T(s), the period.
- V_B(V), the input voltage.

Rewriting this to an expression for the primary inductance results in,

$$L_p \leq \frac{V_B \cdot D \cdot T}{Ip, peak} \tag{2-6}$$

Substituting equation 2-6 into equation 2-4 results in,

$$I_{p,peak} \leq \frac{2 \cdot P_{out}}{V_B \cdot D} \tag{2-7}$$

Taking into account that the input voltage can vary between 12V and 48V and the duty cycle is less then 50 percent, the peak current and number of turns can be calculated.
The number of turns is related to the inductance via the following formula,

$$L_p = n^2 \cdot A_L \tag{2-8}$$

with,

- A_L(H), the inductance factor

The inductance factor is the inductance of the coil when n is equal to 1 and can be found in the datasheet of the core type[7]. Since one of the established requirements is a turns ratio of 1:1, the primary inductance will be equal to the secondary inductance($L_p = L_s = L$). The peak current and the inductance value are important parameters to consider when looking at the duty cycle, since the current rises with a factor $\frac{di}{dt} = V/L$. If it is not able to reach the necessary peak current within it's duty cycle, the desired output power cannot be achieved. Which means that the peak current needs to be raised and/or the inductance needs to be reduced[10]. Taking this data into account a core size is picked with a certain gap length. The number of turns can be calculated and the peak current can be measured. These values are used to check whether the flux density is below 300 mT. When the flux density is above 300 mT, a bigger gap is chosen. When this isn't enough, a bigger core is used. When the flux density has the correct value one has to check if the number of turns needed to gain the specified value of the flux density fits on the core, which could have an effect on the inductance value. Lastly the inductance value is calculated using equation 2-8.

After the steps described above have been done, the winding method needs to be determined and the DC resistance needs to be estimated. The second of which is done using the following equation,

$$R = \frac{\rho \cdot l}{A} \tag{2-9}$$

with,

- R(Ω), the DC resistance of the wire.
- l(m) $= 2\pi \cdot r \cdot n$, the length of the wire.
- A(m^2) $= \pi \cdot r^2$, the surface of the wire.
- $\rho(\Omega \cdot m)$, the resistivity of the material.

Rewriting equation 2-9 gives,

$$R = \rho \cdot \frac{2 \cdot \pi \cdot r_{core} \cdot n}{\pi \cdot r_{wire}^2} \tag{2-10}$$

with,

- r_{core}, the radius of the middle shaft of the core
- r_{wire}, the radius of the wire

With respect to the winding method it is important to decide how many layers are needed. When it is necessary to have multiple layers it is possible to make use of interleaving[5]. Interleaving is a winding method at which the secondary winding is 'interleaved' in between the primary winding. For instance when using four layers, two primary and two secondary, the order of layers would be P-S-S-P. The benefit of this method is that there will be no magnetic field at the boundaries of the different sections.
Based on the given formulas stated above the transformer parameters can be determined.

Component selection As already mentioned the choice has been made to use the E core type. Preferably a core with low leakage and wide windows. A viable option that meets these specifications would be the ETD core. The size can be relatively small for the application it will be designed for. The first core that will be looked at is the ETD29. Basically the smallest ETD core type there is on the market right now. The air gap is taken as big as possible, which in this case is 1 mm. This gives an inductance factor of 124 $\cdot 10^{-9}$ (H/turn) and a core area of 71 $\cdot 10^{-6}(m^2)$
Now that the core type and size is determined the other parameters need to be established in order to check whether the transformer meets the requirements. First of all equation 2-7 is used to determine the peak current before the inductance value is calculated. This value is maximal at a low input voltage of 36V and at an output power of 110 Watt resulting in a peak current of 12.2 Ampere. Using this value the number of turns can be determined using equation 2-1 resulting in n equal to 14 turns. Using equation 2-8 the inductance is determined at 24 uH.
Lastly, the core needs to be winded. Initially the selected material for winding is copper, which has a resistivity of 1.68 $\cdot 10^{-8}$ (Ω·m). Using equation 2-9, a rough estimation of the DC resistance can be made. Using n equal to 14 results in a DC resistance of 5.5 $m\Omega$ over the primary and secondary side. In order to fit the number of turns on the core a wire thickness is picked of 1.25mm. The available space for the winding is equal to 22, dividing 22 by 1.25 equals approximately 17 turns. The transformer consist of one primary layer and one secondary layer. Both winded in the same direction in order to meet the polarity of the transformer.
After the transformer has been winded, the transformer should be connected to the spectrum analyzer. This device determines the inductance value, the leakage inductance and the AC resistance. Section 5.3 describes the results.

Remarks

Skin effect and with it the skin depth are also factors that can be of importance for the transformer. Skin effect is the tendency of AC currents to distribute itself in such a way that the current density at the surface is higher than at the center, see figure 2-6. The parameter δ, called the skin depth, determines how close the current flows along the surface of the conductor[20]. Ideally, all the windings should have a single layer. When using a single layer for both the primary and secondary layer, the layers can be much thicker than the skin depth without adverse effects[18]. The proximity effect should also be mentioned. The proximity effect occurs when an AC current in a conductor causes eddy currents in close by conductors[13].

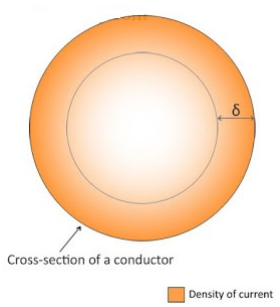

Figure 2-6: Skin effect in a round wire

Both factors need to be taken into account when testing the transformer with the selected wires. For instance, when the AC resistance of the transformer is unexpectedly high perhaps other winding material needs to be used to counteract this.
For the determination of the AC resistance the formula of Dowel can be used. This formula is used since it takes into account, among other elements, the skin effect and the proximity effect[27].

2.2.2 Switching Component

The switching component of a flyback converter is one of the most vulnerable parts within a flyback. For maximum system robustness and reliability a properly rated power MOSFET has to be selected along with a high efficiency. The MOS family has two main branches, the PMOS and the NMOS. The basic functionality is the same, but the operation modes and applications differ between the two. In most cases the NMOS is a better choice due to the orientation of its internal body diode, and better circuit performance and efficiency compared to the PMOS, therefore this type of MOSFET will be used[6]. Things to consider with the selection are; blocking voltage, on-state current, switching frequency, switching losses, internal body diode and more.

Requirements

Besides the requirements stated in 2.3, the specific requirements for the the switching MOSFETs are:

- Breakdown voltage (V_{DSS}) of the MOSFET has to be able to withstand the high voltages encountered during the switch in OFF state (req).
- The maximum drain to source current (I_D) of the MOSFET needs to be rated for the maximum current flowing during the ON state (req).
- The MOSFET has to be robust, meaning being avalanche rated and should be accompanied by fail safe circuits (wish).
- Low power losses within the MOSFET (wish).
- The MOSFET has to be able to switch at 125 KHz (wish).
- Gate-to-source voltage V_{GS} has to be compatible with the PWM controller (req).

Component selection

First step in determining the right switching component or NMOS to choose for a flyback realization is to take a look at the ON and OFF states of our switch. In the ON state, the voltage across the MOSFET drops to nearly zero, current flows linearly into the primary inductor of the transformer and energy gets stored into the transformer. Here the rating to take into consideration is the maximum drain to source current I_D. This would have to be larger than the maximum current flowing in the primary side of the transformer which is for our transformer 12.2A, mentioned in 2.2.1. When the MOSFET turns off, an extremely high voltage is generated across the device as shown in figure 2-7. It is because of this that the break-down voltage V_{DSS} is a crucial parameter to consider in flyback power supply design[24]. This high voltage generated consists of the (maximum) output voltage across the secondary reflected back through the transformer and multiplied by the turns ratio (nVo), (maximum) input voltage (V_{inMAX}) and a spike voltage due to the effects of parasitics caused by the primary leakage inductance (L_{lk1}) and MOSFET output capacitor (C_{oss}) labeled as V_{Lleak} (detailed explaination of this resonance is found in [21]). All these voltages are in series with each other making the calculation for minimum V_{DSS}:

$$V_{DSSmin} = nVo_{MAX} + V_{inMAX} + V_{Lleak} \tag{2-11}$$

For our flyback $nVo_{MAX} + V_{inMAX}$ is around 96V to leave some room for the leakage induction spike a double of the minimum V_{DSS} is recommended. Thus, a V_{DSS} in the range of 150V-200V should be sufficient.

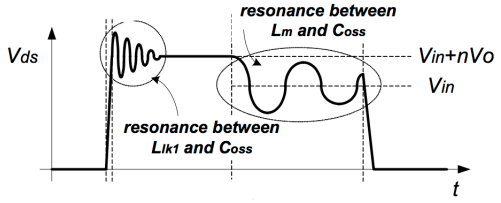

Figure 2-7: Resonance caused during DCM operation [21]

Second step in selecting a MOSFET is to take generated power losses into consideration. The power loss in a MOSFET mostly comes from two sources, the conduction losses and the switching losses. Conduction losses are caused by the resistive element in the MOSFET $R_{DS(on)}$. This element dissipates power as the current is conducted through the MOSFET and is inversely proportional to the size of the device [23]. Also a high V_{DSS} has some influence as these MOSFETs tend to have higher conduction losses [24]. Switching losses, on the other hand, are caused by the output capacitance C_{oss} of the MOSFET. During each switching cycle the energy stored in C_{oss} is dissipated in the MOSFET. Thus, for high switching frequency, a small C_{oss} is preferred. The equations for switching and conduction losses are [23] [34]:

$$P_{switching} = \frac{1}{2} \cdot C_{oss} \cdot V_{DS}^2 \cdot f_{switch} \tag{2-12}$$

$$P_{conduction} = R_{DS(on)} \cdot I_{DS(rms)}^2 \tag{2-13}$$

$$I_{DS(rms)} = I_{p,peak} \cdot \sqrt{\frac{D}{3}} \tag{2-14}$$

$$P_{losses} = P_{switching} + P_{conduction} \tag{2-15}$$

With the considerations mentioned above, the AUIRFR4620 MOSFET was selected. This power MOSFET is automotive qualified to Infineon standards, which makes it low in switching and conduction losses thus making it good for fast switching and operating at high temperatures [14]. It is also rated for repetitive avalanche, which allows the MOSFET to dispense the surge voltage into heat. Together these features contributes to overall system robustness. The relevant datasheet values are the following [29]:

- $V_{DSS} = 200V$
- $I_D = 24A$
- $R_{DS(on)} = 64m\Omega$
- $C_{oss} = 125pF$
- $V_{SD} = 1.3V$
- Operating Temperature of 175 °C
- $V_{GS}(max) = \pm 20V$ with V_{th} = 3-5V

Compared to other power MOSFETs in this V_{DSS} range the AUIRFR4620 has a low output capacitance C_{oss}, yet retains a reasonable $R_{ds(on)}$, leading to lower switching losses considering that the system would be switching at medium-high frequency. Using the functions 2-12, 2-13 and 2-15 this leads to an estimated MOSFET loss of 1.6W assuming the system is running at maximum power output, D = 0.49 and maximum switching frequency of 125 KHz.

Switching Circuit Design

However, a drawback of this MOSFET is that the body diode voltage is considerably high (1.3V). This leads to further losses on the secondary side of the flyback when the MOSFET is in flyback diode mode. To avoid this we placed a schottky-diode (V20202G-M3/4W) in parallel with the MOSFET (figure 2-8) with a lower diode voltage drop of 0.71V. This way most of the current flows through this diode instead of the inefficient MOSFET body diode.

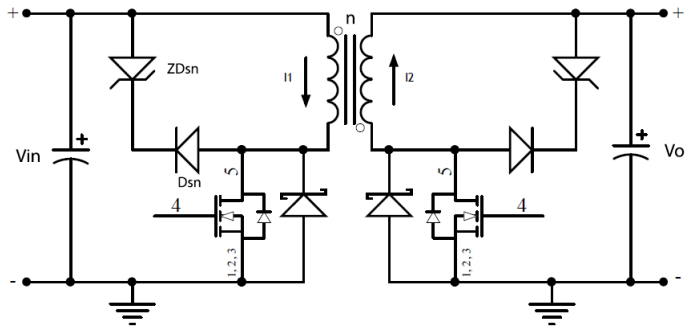

Figure 2-8: Switching circuit adjustments with clamp and schottky

For further robustness of the system it is recommended to ensure that the power MOSFETs will not go into avalanche mode [24]. This is accomplished by adding a clamp circuit over the transformer as shown in figure 2-8. The clamp circuitry considered for our flyback is a zener diode clamp because of its simplicity and amount of component. Clamp circuits absorb the parasitic excessive voltage produced by the leakage inductance. This is accomplished when the clamp diode (D_{sn}) turns on when V_{clamp} exceeds $V_{in} + nVo$. V_z (zener clamp voltage) should be chosen based on a voltage V_{max}, sufficiently lower than the maximum V_{DS} of the MOSFET and the input voltage Vin.

$$V_z = V_{max} - V_{in} \tag{2-16}$$

Making the power dissipated in the zener diode [24]:

$$P_z = \frac{1}{2} L_{leak} \cdot i_{peak}^2 \cdot \frac{V_{clamp}}{V_{clamp} - nV_o} \cdot f_s \tag{2-17}$$

Remarks

Lastly, another factor to take into consideration while selecting a MOSFET is the body package. Different types of packages have their own characteristics. For our application a reasonable sized D-pak (2-9) was chosen due to ease of prototyping, but choosing smaller packages can result in better efficiency performance. Heat dissipation is also something to acknowledge, MOSFETs performance decreases and becomes less efficient at high temperatures. The AUIRFR4620 however has a high operating temperature of 175 °C and a heat sink was not considered necessary in this design, although the option to add one later on has been left open.

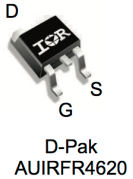

Figure 2-9: AUIRFR4620 [29]

2.2.3 Integrated Circuit PWM controller

There are multiple ways to implement the control of the converter's MOSFETs. One is by using a microcontroller, performing voltage and current measurements and generating a PWM signal based on a PI-controller. The upside of this approach is the degree of freedom when one writes their own code and control loop, and having the ability to use the microcontroller's other peripherals like I^2C, UART, etc. for direct communication, feedback and in-circuit debugging.

Another approach is to use an Integrated Circuit (IC) PWM controller. An IC PWM controller is basically a hardware implementation of a certain control-loop, designed to perform one specific task. The upside in this case is that the entire flyback converter control can be implemented through a single, purchasable IC, and thus reducing the complexity of the control circuit significantly as compared to the microcontroller realization. Therefore, the choice has been made to design our converter with an IC as controlling element. The complexity of the converter and the available time played an important role in the decision. With the IC implementation the converter can be controlled with just a few analog signals that any microcontroller or development board is able to interpret and generate, thus creating a very robust and accessible flyback converter with power management capability.

Requirements

The IC is a crucial component in the design, since it performs all measurements and control of the MOSFETs. The IC must be well-chosen in combination with the switching component, as the collaboration of these two components form the basis of the control system. The IC must be stable, reliable, efficient and easy to control. As the component choice in this case is generally not subject to fundamentally different operating approaches, the IC choice is determined by other characteristics with respect to; control method, working frequencies, operating temperatures, voltage limits and IC packaging, which are variable for each manufacturer and product family. Some actual requirements are:

- Vcc must be above the gate threshold of the MOSFET (req).
- Operating mode must be compatible with our bi-directional flyback topology (req).
- IC must be compatible with the switching of a low-side FET (req).

Design

When seeking for suitable IC's one starts with narrowing the search to a control method applicable to the desired converter topology. For our flyback converter topology the available control methods are: Current control, Voltage control, Feed Forward control, Valley Current control and Peak Current control [17]. All of these methods can be used to control our circuit, so the choice was based on the stability, complexity and accessibility of the control IC. Both current and voltage control are proven, reliable control methods as they are the oldest and most used methods in SMPS design, based on simple PID control loops. Feed Forward is a more recent control method that builds upon the classical PID-controller by adding terms that predict the behaviour of the converter, making the controller proactive instead of reactive. Lastly, Peak current control and Valley current control are two methods that add extra features to the established current-mode control method. Peak current control features an extra control loop based on trailing-edge modulation that senses the current through the inductor and allows an analog signal to set the maximum allowed current. Valley current control adds loss-less current sensing and a leading-edge modulation control loop that makes it suitable for high frequency,

high current buck conversion with small duty cycle variation.

For our converter the peak current control method is an excellent choice. It implements the standard control needed for normal converter operation, and adds current limiting in a robust and accessible manner. Now that the search has been limited to flyback topology, peak current control IC's the choice lies with the last parameters regarding switching frequency, Vin, Vout, gate drive current, and duty cycle limits. Our switching frequency, Vin and Vout are reasonably standard values and any IC will be compatible. Furthermore, the gate drive current does not have to be very large as the MOSFET does not require it when switched in the electrical circumstances of our converter. Lastly, the duty cycle maximum is an added feature that limits the duty cycle to a predetermined value. Choosing this value at 50% is a convenient addition to the converter as it reduces the converter behaviour to purely Discontinuous Current Mode (DCM).

Figure 2-10: PDIP-8 IC

With these design parameters the UCx84x family seemed promising. The final choice landed on the UC2845 by Texas Instruments due to its duty cycle limit, operating temperature and turn-on voltage, making the converter suitable for voltages as low as 12V, which is the standard battery voltage level.

Remarks

The PWM controller IC is a good choice for fast, analog control of our flyback converter. However, care must be taken when designing a PCB because the analog control circuitry is sensitive to noise and consists of a few critical current paths.

2.3 Topology Design

Keeping all previously mentioned subjects in mind, the final converter topology has been designed and the schematic can be found in figure 2-11. The entire schematic, together with all subsystems is depicted in appendix A figure A-1. The essential components needed for the bi-directional functioning of a flyback converter are all present in the form of the transformer, the MOSFETs and capacitors C19/C22.

The switching of the MOSFET introduces noise onto the input and output voltage lines, additional capacitors (C20,C21,C23,C24) have therefore been added to function as high-frequency noise paths to stabilize the output, as well as increase accuracy of the measurements [33].

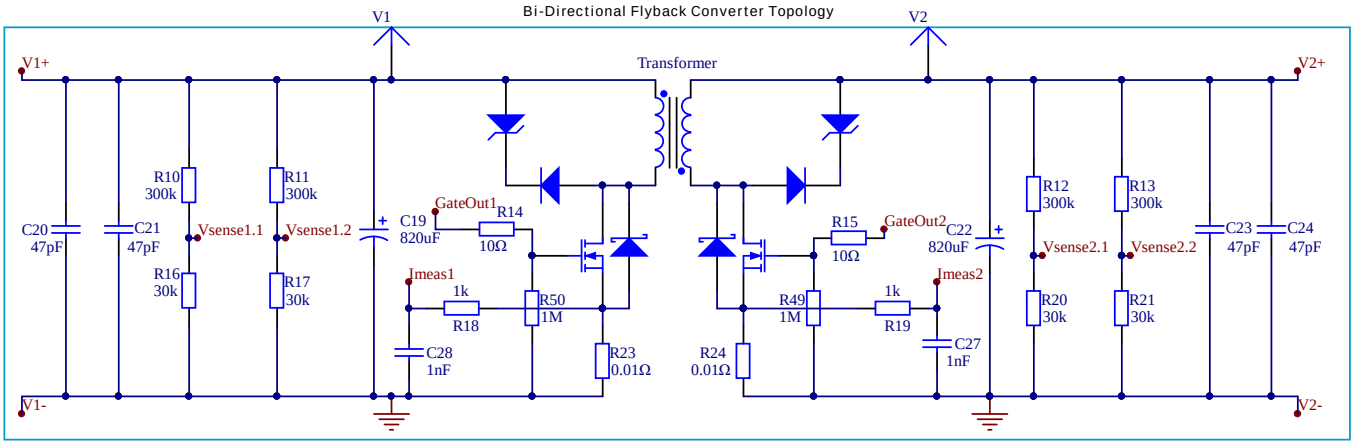

Figure 2-11: Bi-Directional flyback converter topology

R14/R15 are two small resistors added to the MOSFET gates to limit the current on these paths from PWM controller to MOSFET. R50/R49 are two large resistors connected from the MOSFET gates to ground to function as a pull-down path when the MOSFET gate signal is left floating.

The Schottky diodes discussed in section 2.2.2 are present in the design as well.

Voltage measurement Four resistor divider networks (R10/R16, R11/R17, R12/R20, R13/R21) have been added to the V1 and V2 rails to function as voltage measurements. The 300K-30K divider ensures that the entire input and output voltage range gets divided by ten to make it usable for the microcontroller and the other subsystems. (12V-48V $\rightarrow$ 1.2V-4.8V)

Current measurement R23 and R24 are two shunt resistors placed between the source of the MOSFETs and GND, and are used for measuring the primary and secondary current. Since the resistance is so small, all of the current through the MOSFETs will pass through these resistors to ground. The current through the shunts creates a potential difference over the resistors which is directly proportional to the current passing through, making it an ideal place to measure the current. The voltage over the resistor however, is very small compared to the noise of the power line. To counter this, a small low-pass filter (R18/C28 and R19/C27) has been attached to both current measurements to filter out some of this noise.

2.4 Subsystems

2.4.1 Peak Current Mode Controller

The PWM control IC needs some components to be able to function[30]. Figure 2-12 shows the design from our Altium schematic. Both IC circuits are identical, and are the foundation of the bi-directional nature of the converter as they each control one MOSFET. The transistors Q3 and Q4 control which IC is being used, and thus controlling the direction of the energy flow.

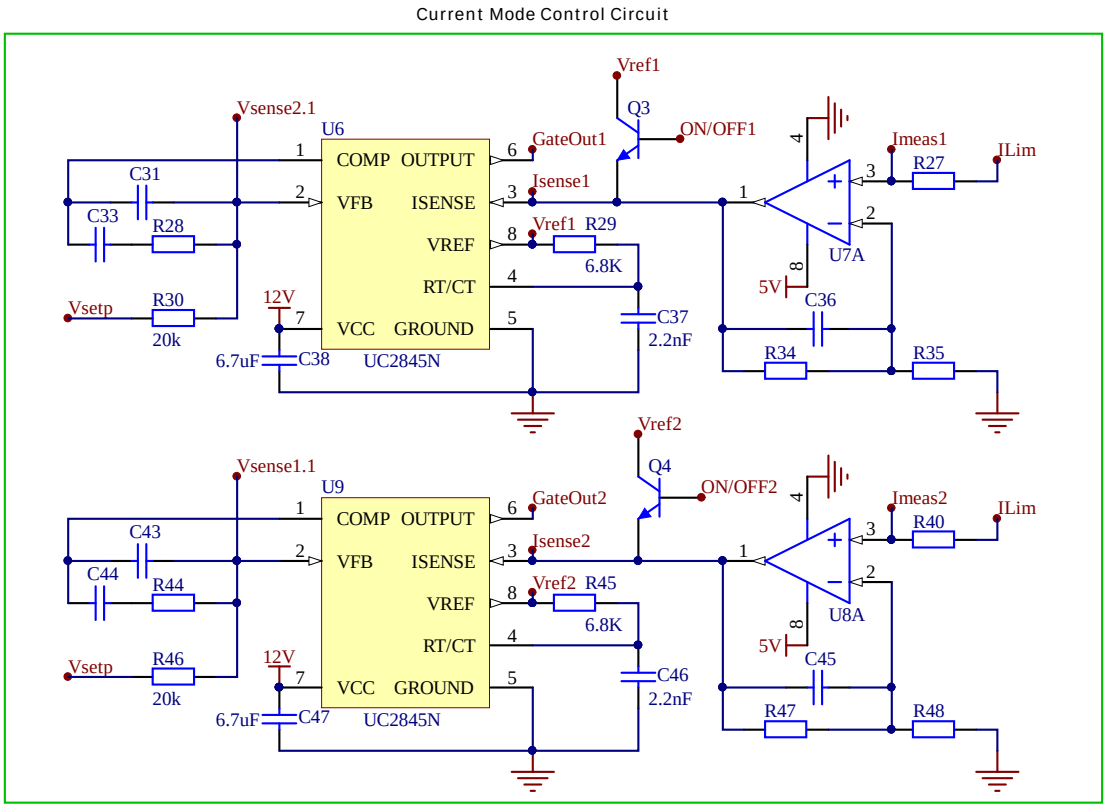

Figure 2-12: Peak Current mode control circuit implementation with UC2845

RT/CT The RT/CT pin of the IC determines the operating frequency of the IC. The resistor and capacitor implementation of R29/C37 and R45/C46 set the IC operating frequency to 125 KHz.

ISENSE The voltage over the shunt resistor is measured and fed into the control circuit through connections *Imeas1* and *Imeas2*. The shunt resistor has a value of 0.01Ω, meaning that a peak current of 20A results in a voltage of 0.2V over the shunt. The IC uses a max. 1V reference voltage, to which it compares *ISENSE* to determine the maximum current. This means an amplifying op-amp circuit is needed to scale the shunt resistor voltage range to max. 1V. This is implemented by U7A and U8A respectively for each side, operating in non-inverting topology. C36 and C45 are added to the feedback network to function as an active low-pass filter to help reduce noise and increase accuracy. The analog current limit signal *ILim*, originating from the microcontroller, is super-positioned onto the current measurement through resistors R27 and R40. This raises the voltage level of the current measurement higher than it actually is, tricking the IC into detecting max current and switching off the MOSFET while the actual current is not actually maximum.

VFB/COMP These pins function as voltage measurements and control inputs. The resistor divided voltage of the output (Vout) is fed into the control circuit through connections *Vsense1.1* and *Vsense2.1*. The components placed between VFB and COMP determine the transfer function of the error amplifier feedback network. The type of compensation and its influence will be discussed in section 3. The analog input signal *Vsetp*, originating from the microcontroller, is super-positioned onto the VFB pin through resistors R30 and R46. If no voltage is applied onto VFB (leave out *Vsetp* and R30), the IC will try to regulate the output voltage so that the VFB pin equals the standard internal value of 2.5V. Depending on the resistor divider ratio on the output this results in a fixed Vout. By adding *Vsetp*, VFB is pushed above or below 2.5V, meaning the IC will regulate the output voltage until VFB is back to 2.5V. Since the resistor divider on the output is no longer a standard 2 resistor network, but has another resistor and an analog signal in the structure (*Vsetp* and R30/R46), the 2.5V at VFB no longer corresponds to only one fixed Vout, but can be any voltage that is within the macro-circuit design parameters.

The **OUTPUT** pin is the signal that goes to the MOSFET gate. This is either 0 V, when the MOSFET should be closed, or VCC (12V) when the MOSFET should be open. The signal is fed through a 10Ω resistor to limit the current spikes of the IC and increase the switching stability.

C38 and C47 function as a local energy buffer for the IC's. When the gate signal is switched from low to high, peak currents up to 1A can flow because the IC wants to turn the MOSFET on as fast as possible. Instead of building a power supply capable of delivering 2×1A to the IC's, the capacitors provide the necessary peak current. The IC's are decoupled from the supply and no longer rely on it for high peak current. A smaller power supply can be used. It is of importance that the capacitor is big enough to provide the current for as long as needed per cycle, whilst also retaining the voltage level of VCC. Choose the capacitor too large though, and the start-up time and current draw increases rapidly.

2.4.2 Measurement Bridge

The measurement bridge is the section of the converter that translates the converter's noisy, analog signals into steady DC signals that the microcontroller can sample with its ADC. The measurements that are of interest to the microcontroller are the voltage and current on both sides of the converter. Figure 2-13 shows the op-amp implementation of these measurements. To measure the voltage, a resistor divider has been placed on both sides of the converter's power traces. This signal is passed to the measurement bridge through *Vsense1.2* and *Vsense2.2*, and fed to voltage-followers U4A and U5A. Note that this is a different resistor divider network as is used for the IC voltage measurement. This is done because the IC forces its resistor divider to 2.5V, thus rendering it useless for the purpose of voltage sensing off-board. R25/C30 and R37/C39 form a passive low-pass filter (LPF). This is implemented to filter out the high frequency switching noise that the converter introduces onto the high-power path.

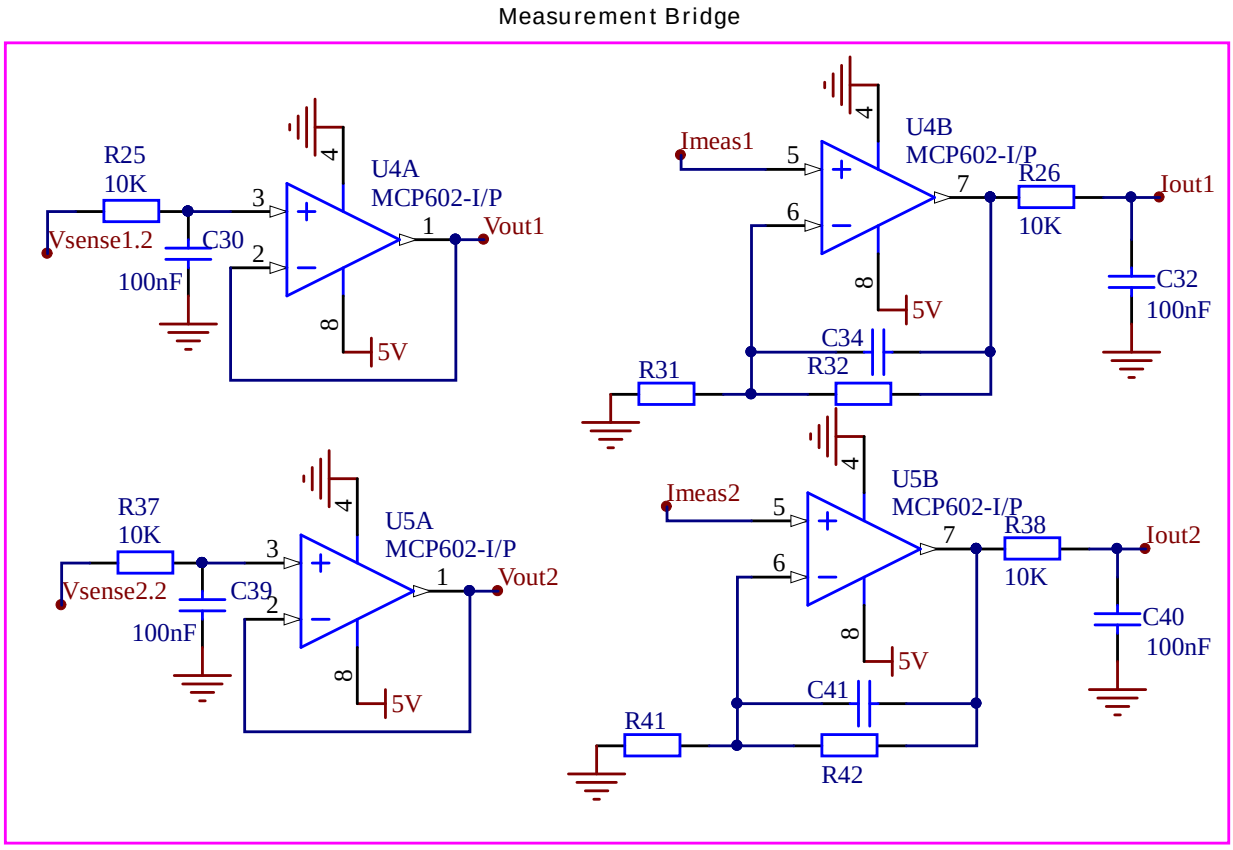

Figure 2-13: Measurement bridge op-amp circuit implementation

The current measurements are done with the same analog signals that are passed to the current mode control circuit, namely *Imeas1* and *Imeas2*. These can be re-purposed for this use because the IC does not force the signal to any value as it does with the voltage sense signals. In order to not disturb the current sense signal, the signal is fed directly into the op-amp without any additional passive filtering. The filtering is done by an active LPF, implemented through C34 and C41, and by a passive LPF directly after the op-amp with R26/C32 and R38/C40. These filters are needed because the current sense signal has the shape of a saw-tooth, while the rms value is the only relevant piece of information. The resistors R31/R32 and R41/R42 provide a non-inverting feedback network that sets a gain for the op-amp, scaling the current sense signal to a value between 0V and 3.3V, which is the input range of the microcontroller's ADC.

2.4.3 Digital to Analog Converter

The Digital to Analog converters (DACs) on the PCB have as function to convert a PWM signal from the microcontroller into a steady DC signal. The reason behind this is that not all microcontrollers have analog output capabilities, while most do have PWM outputs. The circuit represents a comparator that compares the PWM signal to 1.56V. The comparator is fed with 5V, thus producing the same PWM signal at the output, but switching between 0V and 5V instead of the normal 3.3V that most microcontrollers use. The PWM is passed through a LPF that smooths the PWM signal to a steady voltage between 0V and 5V, depending on the duty cycle of the signal.

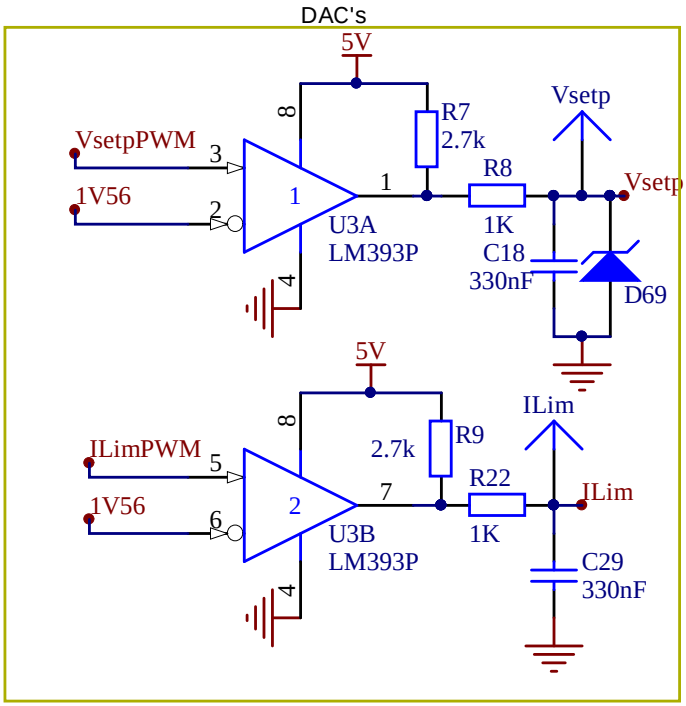

Figure 2-14: Digital to Analog circuit implementation

This implementation allows the converter to be controlled by almost any PWM signal which is present on nearly all microcontrollers, and the generation of the DC signal is independent of the voltage of the PWM signal, as long as its digital high is above 1.56V. The zener diode D69 has been added to add the feature to limit *Vsetp*, and thus Vout, in hardware on the converter itself, adding another level of safety.

2.4.4 Direction Comparator

The direction comparator section of the converter takes a digital signal from the microcontroller (0V or 3V) and converts it into two inverted signals (0V or 5V) used to control the transistors Q3 and Q4 in the current mode control circuit, described in subsection 2.4.1. This way the microcontroller can determine the energy flow direction of the converter by the use of a single digital output signal.

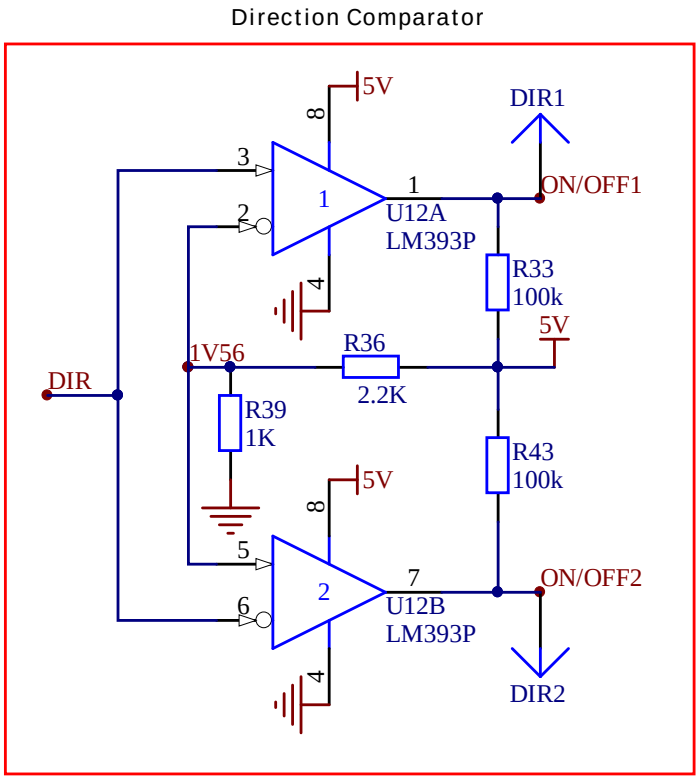

Figure 2-15: Direction signal comparator implementation

The 1.56V compare voltage is generated using a resistor divider network of 2.2K and 1K, implemented through R36 and R39. The digital signal is fed into a different input of either comparator, ensuring that the output signals **ON/OFF1** and **ON/OFF2** are inverted. R33 and R43 function as pull-up resistors for the comparator as these do not have any internal pull-ups.

2.4.5 Power Supply

The voltages needed for the converter subsystems are 12V and 5V. Both of these are generated by the power distribution section of the converter. The LM2575HVT IC family is used as they have a large input voltage range and an easy direct feedback network, which makes it easy to implement. Specific models used are the LM2575HVT-12 and LM2575HVT-5, corresponding to the 12V and 5V direct feedback variant of the general IC family. The IC's inputs are connected through diodes to both sides of the converters high-power path. This results in the power distribution being fed from whichever of the sides has the highest voltage, negating the need for a separate power input. The large input range of the IC's also ensures that the converter can be powered throughout the whole input and output range specifications of 12V to 48V.

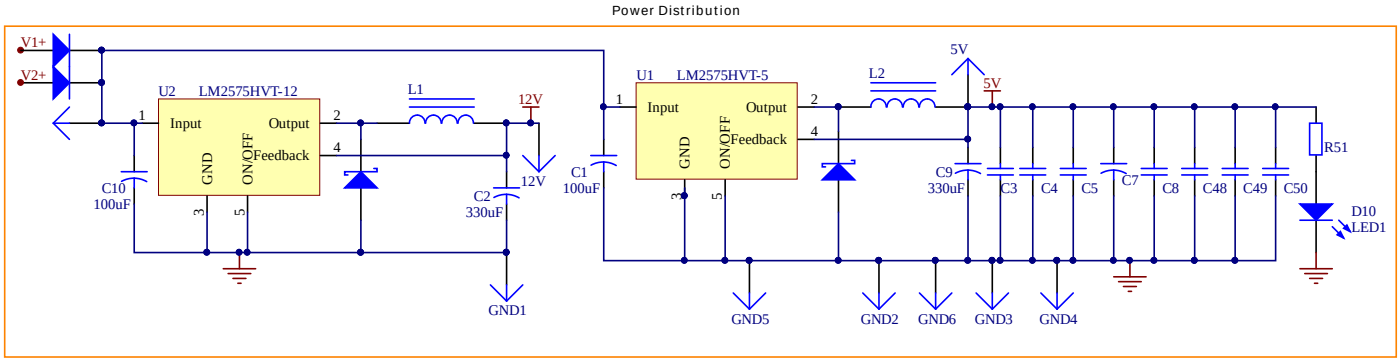

Figure 2-16: Power supply IC implementation

The IC has a built in switching component, and together with a diode, inductor and capacitor on the output it forms a simple and robust buck-converter [31]. A LED has been added on the 5V rail to serve as visual feedback on the power state of the converter. The capacitors on the 5V rail serve as bypass capacitors for all the other subsystems working with 5V [33].

2.5 Use

Initially, the flyback converter is designed for the eBike solar charging station located at the campus of the TU Delft. The charging station next to the EEMCS tower is equipped with 8 solar panels, capable of a total peak power of 2.3 kW, see figure 2-17 [19]. The flyback converter will be a small but important link in this chain, capable of regulating a load voltage and limiting the output current, while being fed from an input DC voltage varying between 36V and 48V. The regulating and bi-directional aspect is put in place in order to make the converter applicable in other areas as well, for instance DC microgrids.

The implemented control and measurement signals ensure easy operation of the converter when integrated into a larger system. For an example of the control network, the thesis "Control Network of Bi-Directional DC/DC Converters" by BAP group B1 can be consulted [35]. The proposed control network features a slave in the form of the Olimex LPC1343 development board, and the master as an ODROID C1+. The control network design use is best illustrated with the intended functionality of charging eBikes. A user deposits their eBike at the charging station and accesses a website used for tracking and controlling the charging functionalities. Any command sent by the user is passed on through server, master and slave, to finally arrive at the the corresponding converter. All measurements are readily available to the user, unbounded of location.

Figure 2-17: eBike solar charging station

Simulations

3.1 Uni-directional

To illustrate the workings of a flyback converter implementation with the UC2845 IC, a simpler, uni-directional simulation has been provided in figure 3-1. This circuit topology consists of the switching MOSFET on the primary side of the circuit, and the MOSFET on the secondary side acting as the flyback diode. The voltage set-point and current limit have been left out to focus on the fundamental operation first. The working of the simulated UC3842 is identical to the UC2845.

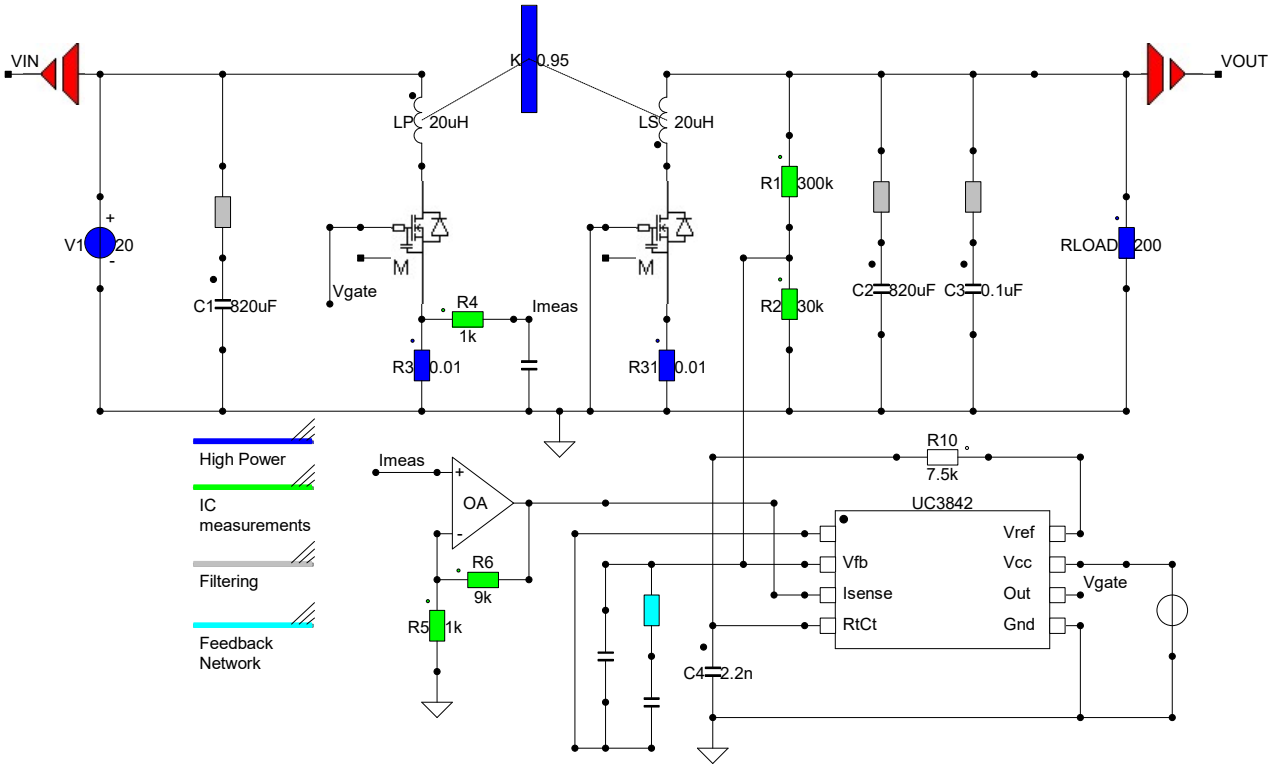

Figure 3-1: Uni-directional flyback converter implementation with UC2845

Figure 3-2 shows the gate signal, output of the IC, and the Isense signal, input of the IC. The IC will generate a PWM signal of a certain frequency according to the resistor and capacitor values R10/C4. The duty cycle is internally limited to 50% for ease of operation. The internal error amplifier and PWM comparator determine the duty cycle of the PWM signal through the measurements of the voltage at Vfb and the shunt resistor ($R3$) voltage at Isense. Figure 3-2 evidently shows the gate signal falling to zero when the current measurement at Isense equals 1V. A simulation of the block diagram can be seen in appendix A figure A-3.

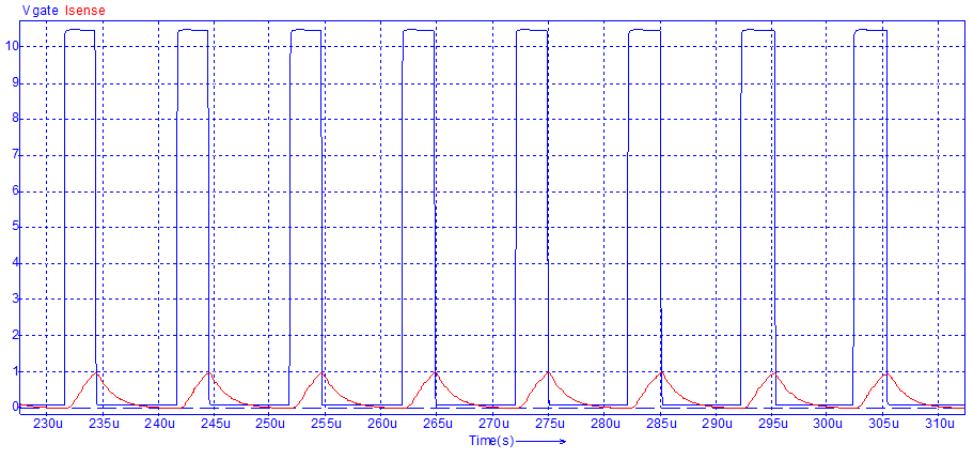

Figure 3-2: UC2845 MOSFET gate signal regulating.

Figure 3-3 shows the start-up of the converter. The current is not limited, and the voltage set-point has not been attached. The distinction can be made between the start-up and regulated load scenarios. When the IC does not measure its desired voltage output, it will allow maximum current to flow until the voltage rises enough to fulfill that criteria (*0-5ms*). When the voltage demand has been met, the IC will actively keep the voltage level steady while supplying current to the load (*5-10ms*). In this operating mode the IC will supply as much current as needed by the load until it reaches its maximum, which is set by the current limit.

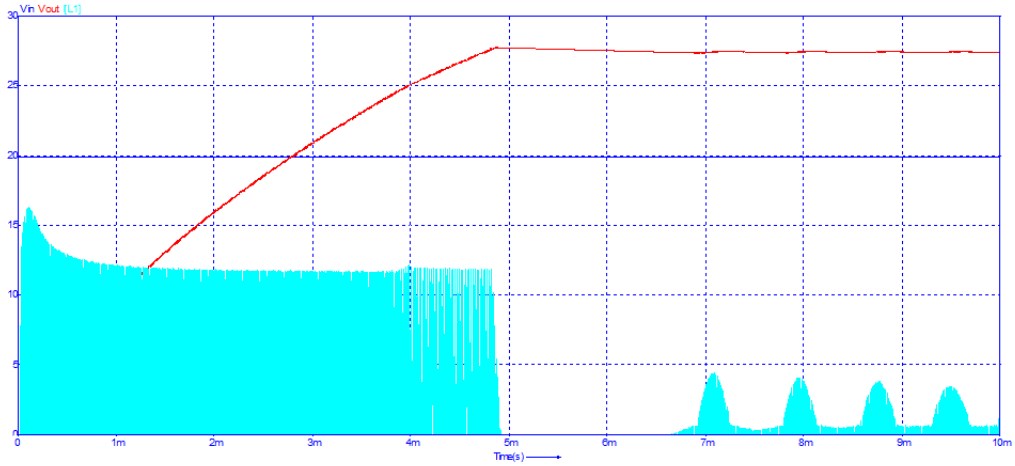

Figure 3-3: Power converter start-up and regulated load electrical characteristics.

Although the design of the feedback compensation network of the IC isn't the main objective of this thesis, it is still of considerable importance to the functioning of the converter. The task of the feedback compensation network is to shape the loop gain such that it has a crossover frequency at a desired place with enough phase and gain margins for good dynamic response, line and load regulation, and stability [15]. For this bi-directional flyback converter a type-II compensation network is more than sufficient, with an integrator, one pole, and one zero. The values of the compensation network determine the actual transfer function parameters and should be calculated to achieve the desired cross-over frequency and gain- and phase-margin [16]. Figures 3-4 and 3-5 show the difference between a well-calculated feedback compensation network and a poorly-chosen one.

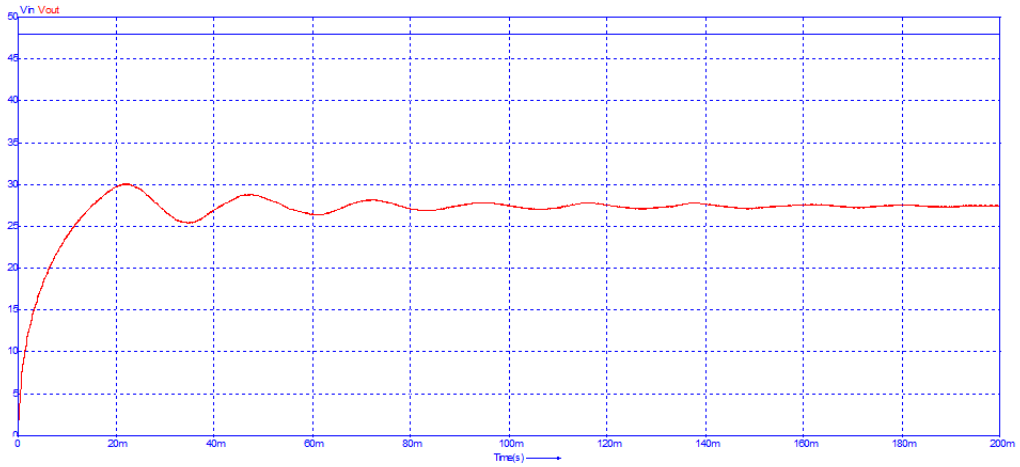

Figure 3-4: Settling characteristics of regulating IC with poorly-chosen feedback compensation network.

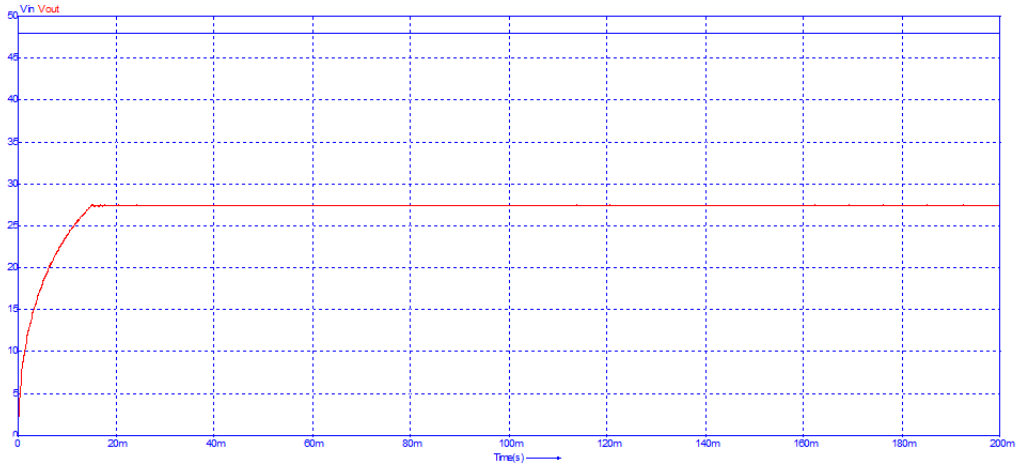

Figure 3-5: Settling characteristics of regulating IC with well-chosen feedback compensation network.

3.2 Bi-directional

Figure 3-6 illustrates the bi-directional implementation of the converter. A second UC2845 and corresponding circuitry has been added, as well as a NPN transistor on both *Isense* lines. The signal **DIR** is provided to the base of one transistor, while the inverted signal **notDIR** is provided to the other transistor. This ensures that only one IC will be active at all times, and the other will be inactive as *Isense* is pulled to *Vref*.

Lastly, the voltage set-point and current limit have been implemented in the form of *V5* and *V6*. The signals are applied to both IC's, as they are only of influence on the active IC.

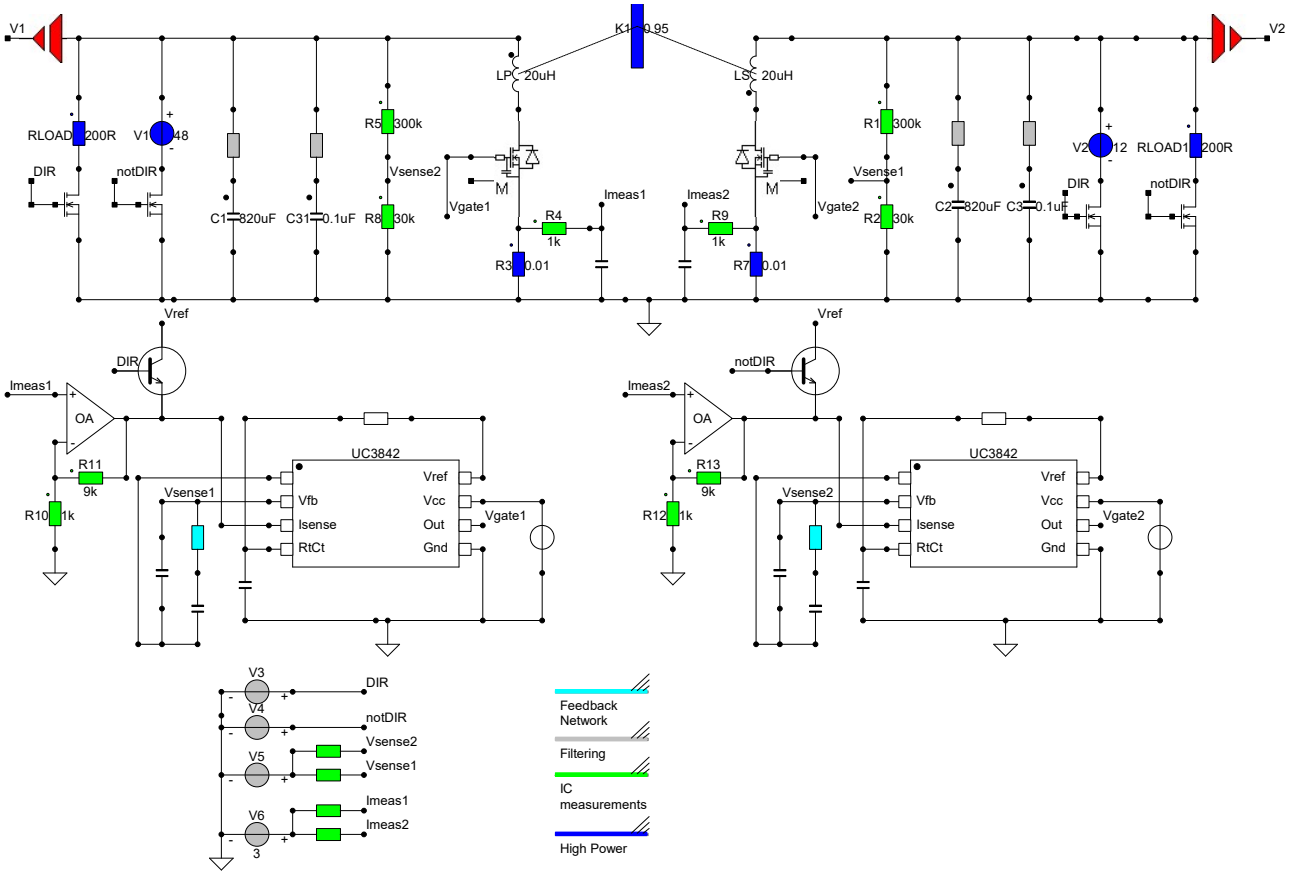

Figure 3-6: Bi-directional flyback converter implementation with UC2845

Figure 3-7 is a simulation of the converter switching energy direction. The direction signal is alternated, periodically switching source and load side, as well as the active IC. Evident in the simulation is the alternating current direction and the corresponding load voltage regulation.

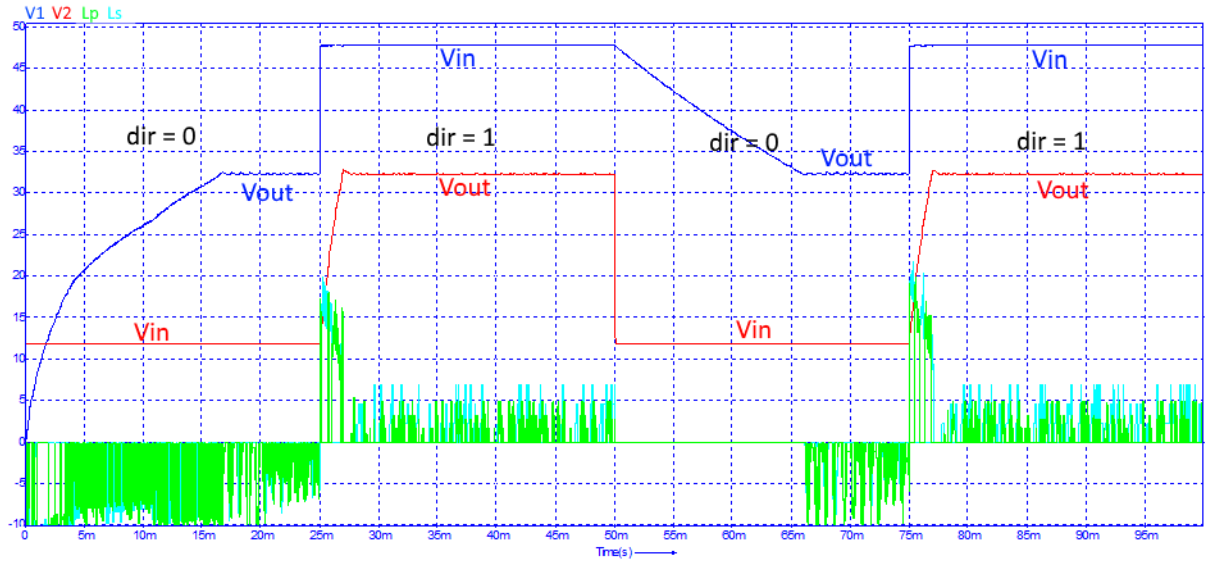

Figure 3-7: Alternating energy direction in bi-directional flyback converter

PCB Design

Printed Circuit Board (PCB) layout is important for switch-mode power supplies since there are high switching currents and sensitive control signals in the vicinity. A well-designed PCB leads to better performance, lower cost, higher reliability and reduced electromagnetic interference(EMI). There are a couple of general guidelines that have to be met: the current carrying traces must be as thick, short and direct as possible, the board must have a low-impedance ground and sensitive signals must be shielded from interference by noisy traces[11].

4.1 Design Layout

There are a few critical current paths in our flyback converter. An overview of the entire layout can be found in Appendix A figure A-2. The high power traces and transformer connection pads are critical to the working of the switching converter. Some of these traces have high $\frac{di}{dt}$ and $\frac{dv}{dt}$ originating from pulsating currents, while others have high RMS continuous current. These traces will introduce a significant amount of noise if not filtered and handled correctly. The high $\frac{dv}{dt}$ traces and the transformers will also contribute considerably to the generated EMI. Therefore, these are ideally placed well away from sensitive, analog signals on-board, as well as away from the microcontroller board. An illustration of these paths and the PCB implementation on our converter can be seen in figure 4-1 and figure 4-2, respectively.
Both the pulsating and continuous current traces are placed distant from other sensitive, analog control signals. Furthermore, the traces consist of big copper pads to more effectively manage higher currents by providing a larger thermal mass and less resistance. The ground connection is done through a ground plane on the bottom layer. Due to this layout, there are four inevitable measurement hazards, encircled blue in figure 4-2, where the measurement will pick up extra noise due to the noisy ground plane directly underneath it.

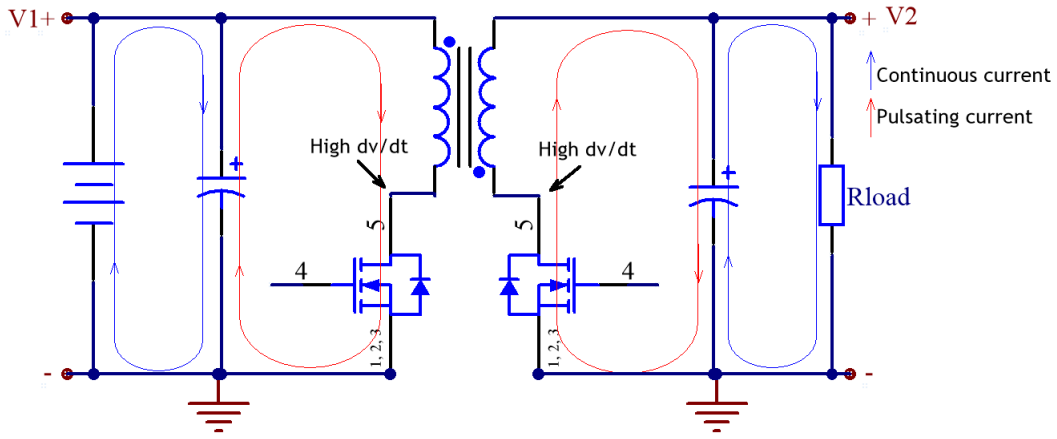

Figure 4-1: Pulsating and continuous current paths in flyback converter

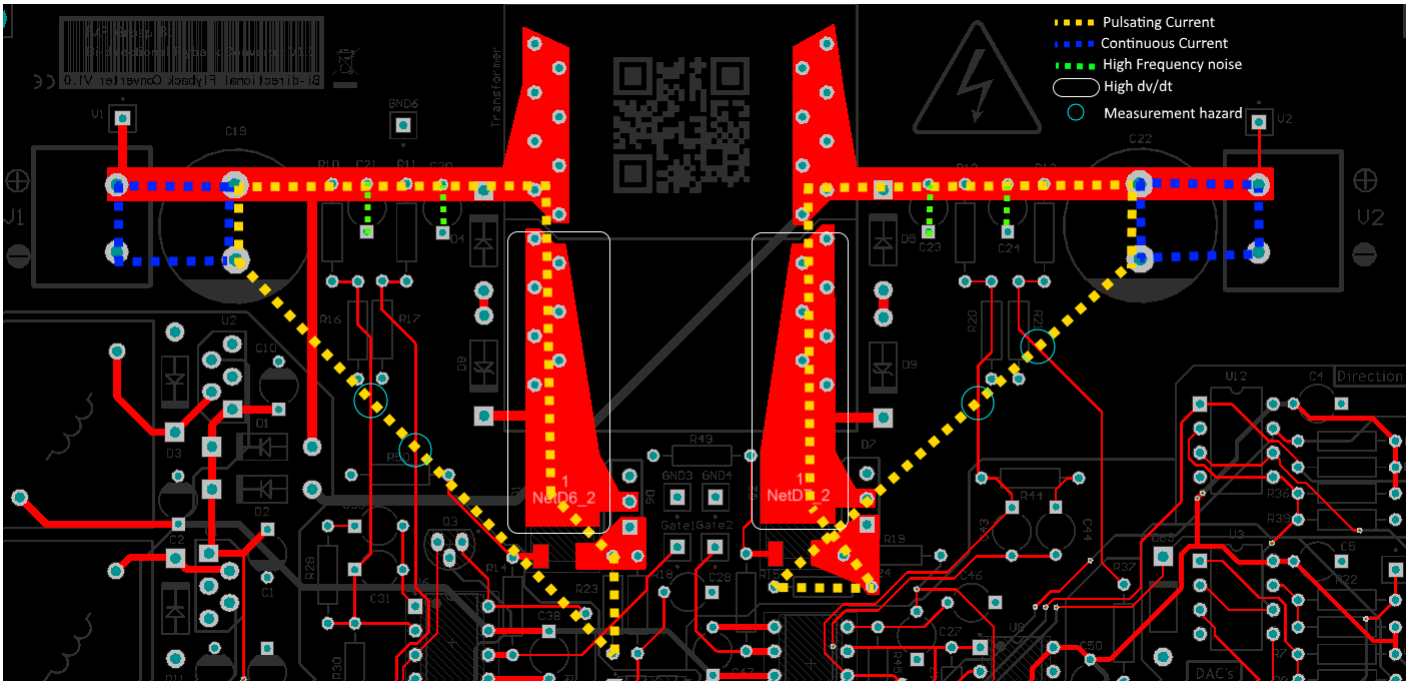

Figure 4-2: Pulsating and continuous current paths in flyback converter PCB

Another critical current path is the MOSFET gate signal path. The IC decides whether to turn on or off the MOSFET depending on the internal circuitry. If the IC decides to turn the MOSFET on, it will try to do so as fast as possible. If no gate resistance is used, the IC's output is not current limited and might result in an unstable system. The current peaks up to 500mA that the IC draws when opening the gate are drawn from the bypass capacitor C38, which is therefore placed close to the IC's pins. The current is returned to the IC through the shunt resistor and the ground plane. Ideally this path is as short and compact as possible to reduce noise picked up by the current loop and increase stability [28].

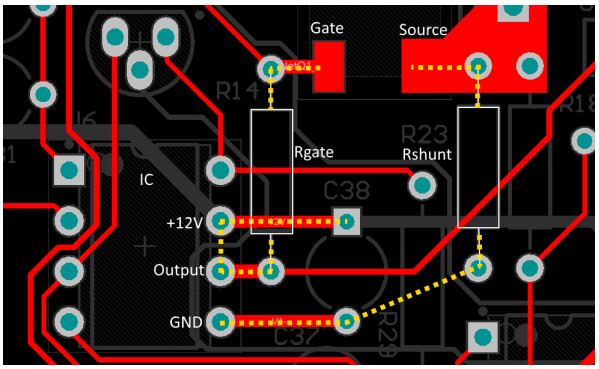

Figure 4-3: MOSFET gate signal current return path

Evaluation

5.1 Overview

In order to test the design of the flyback converter a testplan was made. The main goal is to check whether the requirements stated in section 1.3 are met. However, before the requirements can be looked at, it is important to populate and test the design's subsystems independently, before looking at the system performance as a whole.

First of all, the components of the power supply are placed on the PCB. To check whether the 5V and 12V line are working properly, the test-points 5V and 12V are used. When this part functions adequately the peak current mode control subsystem of both sides, including the MOSFETs are soldered onto the PCB. Here the gate of both the MOSFETs are measured to verify whether the gate receives the expected PWM signal of around 12V. This is initially done while the current(*Ilim*) and voltage(*Vsetp*) are not connected. After this the transformer and clamp circuit are placed on the PCB. This is the first time to check whether the regulating part is working correctly. Since the voltage setpoint isn't connected the output is supposed to take on a constant value based on the voltage divider, described in section 2.1.

When the systems above are all working properly the other subsystems, described in section 2.4 can be soldered onto the PCB. First, the direction comparator is connected, as already described this subsystem has the function to control the direction of charging for the flyback. To check this the test-points DIR1 and DIR2 can be consulted, and based on the value of these pins one of the IC's needs to be turned off, while the other is in normal operation.

Secondly, the DAC is put in place. A reference PWM signal should be provided to check the low pass filter of this system. Lastly, the measurement bridge is verified. To check whether the system is working properly the scale reduction and noise filtering needs to be checked.

If the board's elements and subsystems are all working, the next step is verifying the requirements. To serve as input and outputs of the converter, a power supply capable of 0-48V/3A is required, as well as some sort of dummy load as an electronic load or variable power resistor for the output.

First of all, the large input/output voltage range and current limiting needs to be tested. This is done by supplying the input with a voltage that is slowly increased from 0V to 48V. The converter needs to switch on at 12V. A voltage between 0 and 5V is supplied to *Vsetp* in order to check the output voltage range. The current limiting needs to be tested by supplying an analog signal to *ILim*. Other design specific requirements can be validated by checking various critical voltage signals as the shunt resistor voltage and the drain source voltage over the MOSFETs, as well as measuring overall system performance and efficiency

5.2 Prototype

Figure 5-1 shows the prototype of the bi-directional flyback converter. The prototype consists of the elements described in chapters 2 and 4. The input and output can be found at the 2 screw terminals(A). The key components as described in chapter 2 are found near the center of the board. The MOSFETs(B), the transformer(C) and the ICs(D) are all placed relatively close to each other. The subsystems are placed around these key elements. The power supply is placed on the left side of the PCB(E), the measurement bridge can be found at (F), the direction comparator can be found at (G) and the Digital to Analog converter can be found at (H).

The prototype has a couple of items that should be mentioned before delving further into evaluation of the circuit. First of all, the ground plane is missing, meaning that the ground connections of the components needed to be soldered manually. Secondly, some footprints appeared to be too small. This involved the shunt resistor, power supply capacitors and the transformer. Thirdly, the prototype uses simple headers to connect the converter with the microcontroller, which isn't preferable when looking at mass production. Lastly, connections of *Vsense1.1* and *Vsense2.1* were switched and the placement of some test-points are odd.

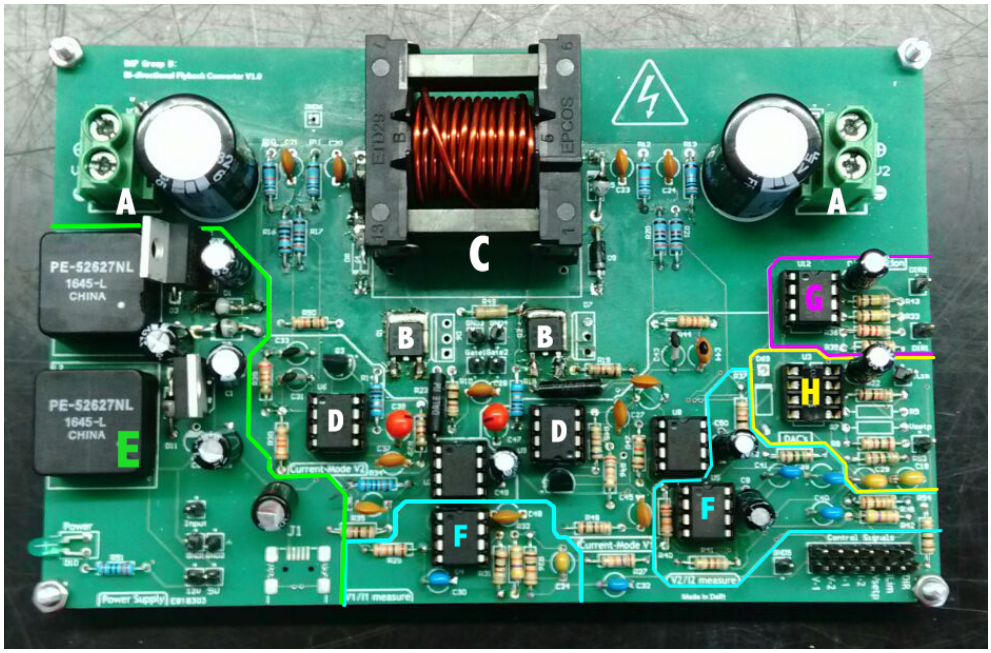

Figure 5-1: Prototype of the flyback converter

5.3 Testing and Results

The design requirements of section 1.3 are evaluated in this section and the results of the transformer are shown.

Transformer results A transformer was winded according to the design described in section 2.2.1. Using an impedance spectrum analyzer both the inductance, leakage inductance and AC resistance of both sides were measured. In the appendix the figures regarding these results can be found. The primary inductance was measured at 19.49 uH, the primary resistance at 340 $m\Omega$, the secondary inductance was measured at 19.77 uH and the secondary resistance at 402mΩ.
To measure the leakage inductance the secondary side of the transformer was short circuited as shown in figure 5-2. This way the reflected voltage is zero and the inductance measured is the leakage inductance. Same can be done for the secondary leakage inductance. The measurement resulted in $L_{lk1} = 389,3nH$ and $L_{lk2} = 390,4nH$.

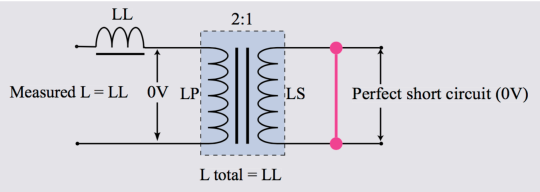

Figure 5-2: Measurement circuit for leakage inductance [26].

Voltage range and Current limit One of the first requirements to test is the large input and output voltage range. In order to be able to charge a variety of different batteries, as well as provide versatility in application the range requirement was chosen from 12V to 48V. Ideally, the switching noise produced by the converter topology is filtered out as well. The converter starts up when either one of the sides is fed with a voltage higher than 12V. The voltage applied to the *Vsetp* input subsequently determines the output voltage that the IC regulates to. Figures 5-3 and 5-4 show the input and output voltage lines. Evident is that the range requirement has been met and it has been determined that the range is controllable with an analog signal between 0 and 5V. The ripple in the output voltage line is limited to an acceptable level, which is a decent result.

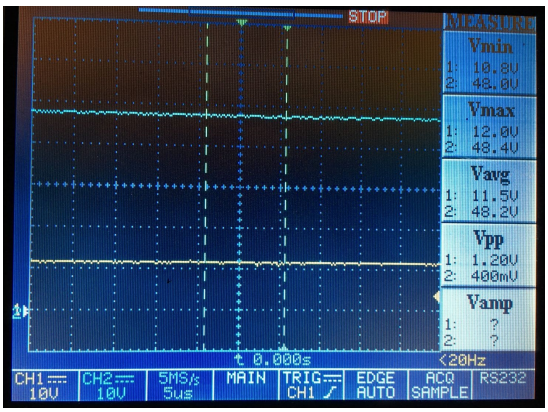

Figure 5-3: Vin=48V, Vout=12V

Figure 5-4: Vin=12V, Vout=48V

The current limit signal has been tested by connecting an analog DC signal to the *ILim* input of the converter. The DC signal is super positioned onto the current measurement entering the IC. The current is successfully limited, and consequentially the converter does not turn on when the limit is set to minimum.

DCM operation The second requirement to test is the discontinuous operating mode of the converter. This can be examined by looking at the current sense voltages over both shunt resistors.

Figure 5-5 shows these voltages with corresponding current axis. Yellow represents the primary inductor current, and blue the secondary inductor current. The switching frequency is 125kHz, the duty cycle is 50% (max) and the input and output voltages are 24V and 48V respectively. The secondary current drops to zero well before the cycle ends, and thus the converter is working in DCM. The signal is very noise, which is probably due to a combination of factors including the ground plane, the measurement tools and the overall PCB layout. According to equation 2-5: $I_{p,peak} = \frac{Vin \cdot D}{Lp \cdot f} = \frac{24V \cdot 0.5}{20uH \cdot 125kHz} = 4.8A$

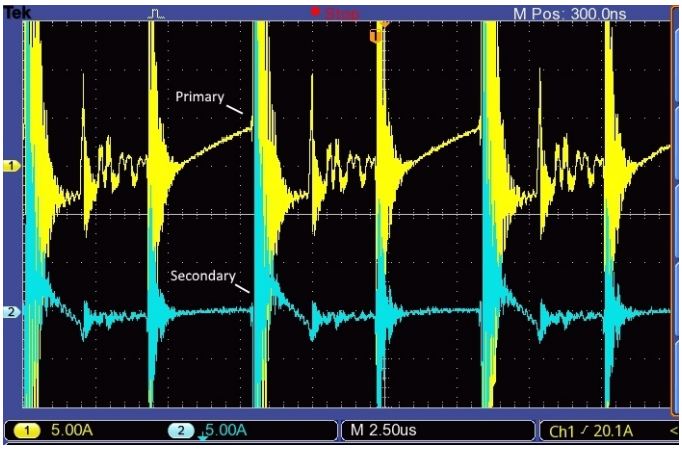

Figure 5-5: DCM operation, Vin=24V, Vout=48V

Which coincides with the actual current entering the primary inductor. If the K-factor was 1, $I_{p,peak}$ would equal $I_{s,peak}$ with the specifications of our transformer, $N1 = N2$ and $Lp = Ls$. This would result in a current fall-time duty cycle of:

$$D = \frac{I_{s,peak} \cdot Ls \cdot f}{Vout} = \frac{4.8A \cdot 20uH \cdot 125kHz}{48V} = 0.25$$

Subsequently, one would expect an RMS current at the secondary side of [34]:

$$I_{RMS} = I_{s,peak} \cdot \sqrt{\frac{t_1}{3T}} = I_{s,peak} \cdot \sqrt{\frac{D}{3}} = 1.39A \tag{5-1}$$

Although the results show a promising waveform, $I_{s,peak}$ and D are not quite equal to the calculated value. It can be concluded that the K-factor is probably not unity, the turns ratio not equal to 1 and the primary and secondary inductance not equivalent. This is a result of the manual winding of the transformer.

Switching frequency The IC output gate signal and corresponding current sense input can be seen in figure 5-6. The IC has no trouble with a switching frequency of 125kHz, thus meeting one of our wishes. The cause of the noise on the gate signal when it is low has not been found yet, but the culprit is probably the bad ground connections and a too large pull-down resistor on the gate.

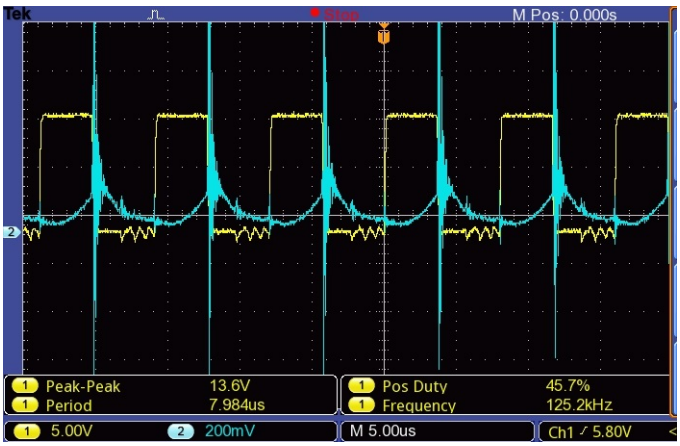

Figure 5-6: Vgs output and current sense signal

The current sense signal corresponds to the simulated signal in section 3 figure 3-2. Once again the noise during switching is extremely high due to the ground connections among possible other origins, the active filter however does filter out a significant amount of the noise, if compared to figure 5-5. In this measurement the current does not exceed the maximum allowed current, and consequentially the IC outputs a maximum duty cycle PWM.

Power output The available power and voltage range of the converter largely determines the functionality and relevance of the product. As a requirement we wanted our converter to be able to deliver at least 110W/48V. The obvious test to perform to measure the power performance is to load the converter while the output voltage is set to 48V. Figure 5-7 shows the measured I-V curve of this trial.

Evident is that the converter does not perform up to the required 110W (48V $\times$ 2A = 96W). As the current goes up, it reaches a point where the IC can no longer regulate the output to 48V, and the output voltage starts to drop according to current drawn. The reason for this voltage drop is that the IC is at its maximum duty cycle limit of 50%, so the power transfer from primary to secondary side can no longer increase without increasing the input voltage. Using the equations for power transfer in a flyback converter stated in section 2.2.1 and equation 5-1, one can calculate the RMS output current at which the power transfer should saturate.

Our calculated RMS current and corresponding power output far exceeds the actual performance. Thus, the RMS current at the secondary side is lower than expected, with a given input voltage and 50% max duty cycle. The cause of this problem could be a number of things. First off, the current entering the primary inductor during the ON-state could be less than predicted, resulting in an overall lower power transfer saturation limit.
Secondly, the resulting current in the secondary inductor during the OFF-state could also prove to be less than calculated. This could be caused by unforeseen losses in the transformer or MOSFET, or a higher secondary inductance than calculated and measured. This, in turn, would also explain the lower power transfer saturation of the converter.

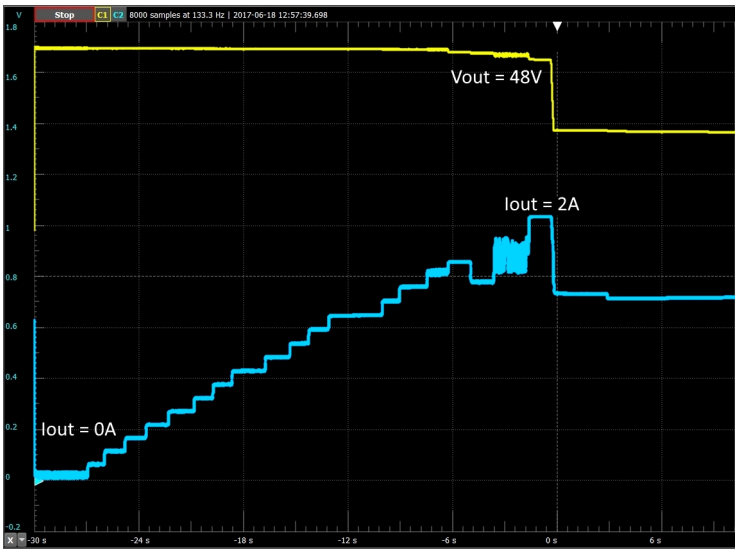

Figure 5-7: Power transfer saturation, Vin=48V

Start-up and output signals The start-up procedure simulated in section 2-15 figure 3-3 was reproduced during a test with the actual converter and can be seen in figures 5-8 and 5-9. The measurements were done on the analog output signals destined to connect to a micro-controller. The measurement bridge does its job and the analog voltage measurement signals (yellow) are fairly stable and noise-free. The analog current measurement signals (blue) are quite stable as well, filtering and amplifying the current sense voltages of figure 5-5. Evident in the start-up figures is the output voltage being regulated to its final value, with a current peak coinciding with the rising edge of the output voltage. After the settling of the voltage, the nominal output current drops to a constant 0.2A. This clearly shows the likeness of the actual start-up behaviour to the simulated behaviour. The secondary current measurement (I2) does not function as expected.

Vin=V1, Vout=V2

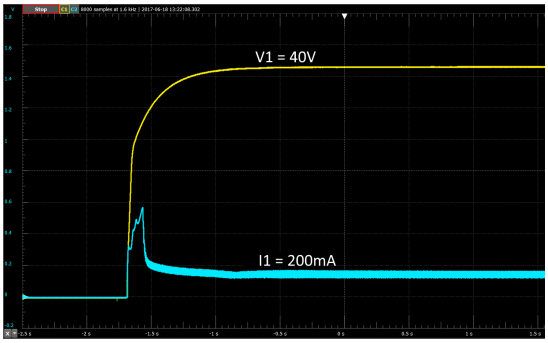

Figure 5-8: Start-up behaviour, V1/I1

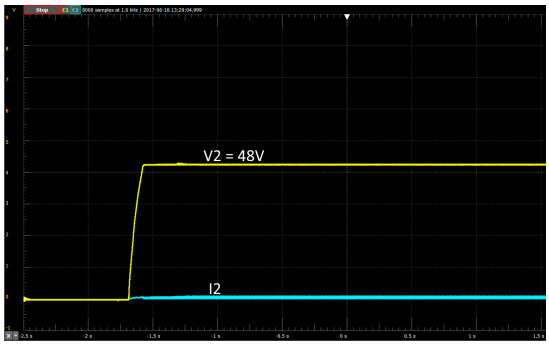

Figure 5-9: Start-up behaviour, V2/I2

Bi-directional functionality A major driving force behind a large part of our converter design was the bi-directional power transfer functionality. To realize this on the converter PCB, both ICs and MOSFETs have to work identically, the power transfer in the transformer should behave independent of direction, and the generated direction signal should turn off one of the IC's while relinquishing control of the other. Figures 5-10 and 5-11 show the same start-up measurements as figure 5-8 and 5-9, but performed in the other direction. Evident is the duality between V1/V2 and I1/I2, clearly illustrating the bi-directional functionality.

Vin=V2, Vout=V1

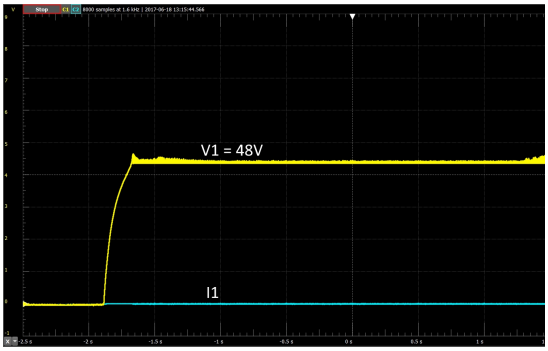

Figure 5-10: Start-up behaviour, V1/I1

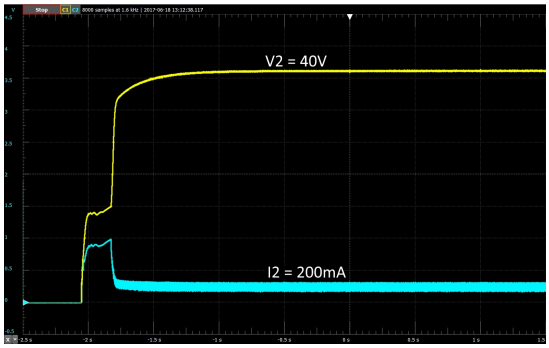

Figure 5-11: Start-up behaviour, V2/I2

Controllability and Application The converter was designed in such a way that it would be controllable by any type of microcontroller, and was also stated as a requirement in section 1.3. The analog measurement output signals from the measurement bridge have been discussed and deemed functioning. The direction comparator subsystem has been tested and considered working. The last signal translation block is the DAC. Figures 5-12 and 5-13 show the DAC's working, smoothing out the *ILim* and *Vsetp* PWM signals to a steady DC-value between 0 and 5V. The converter functions as expected with the DC control signals.

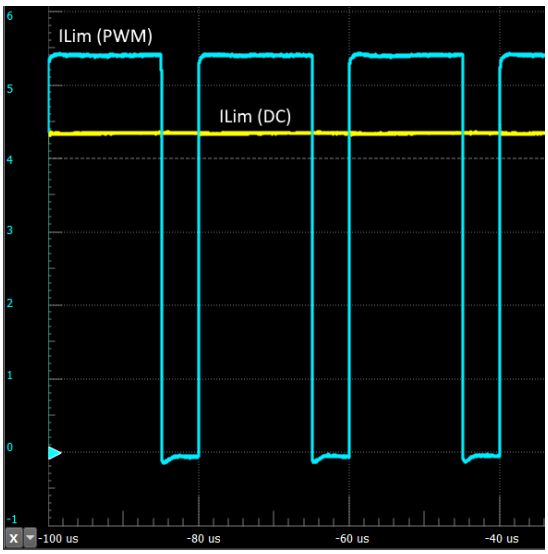

Figure 5-12: DAC of *ILim*

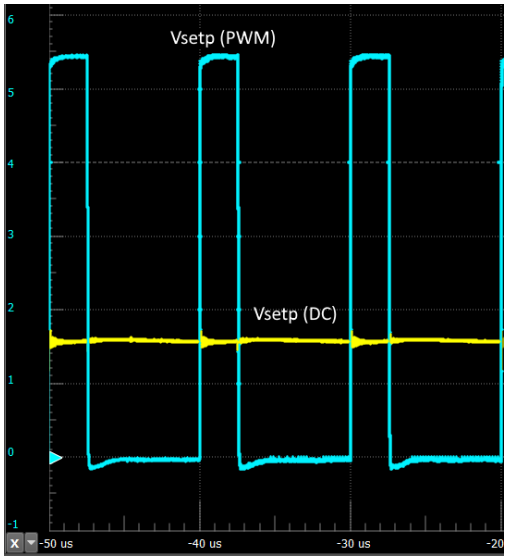

Figure 5-13: DAC of *Vsetp*

This feature together with the bi-directionality satisfies another wish stated, which was that the converter is applicable in a variety of different circumstances, such as DC-smart grids or the automotive industry. The relatively easy control makes the converter suitable for low-cost, highly-integrated smart DC-grids, as well as for novel, high-speed power control in automotive vehicles. The power output however, limits the functionality significantly.

Robustness and Durability A critical parameter and driving force of the design of the flyback converter as stated in section 2.2.2, is the V_{ds} over each MOSFET. Figure 5-14 shows the characteristic voltages during multiple switching cycles of our converter. The converter was tested with maximum electrical conditions of Vin = 48V and Vout = 48V, where the reflected V_{ds} on the switching MOSFET is highest (blue curve). The peak voltage measured is 154V, and occurs right after switching off the MOSFET. This is also the peak that one wants to clamp for a robust system. In our case, the chosen MOSFET can easily withstand this voltage and we have therefore tested it without the clamp circuit in place. For robustness it could be considered to place the clamp circuit anyway, as this adds another level of safety.

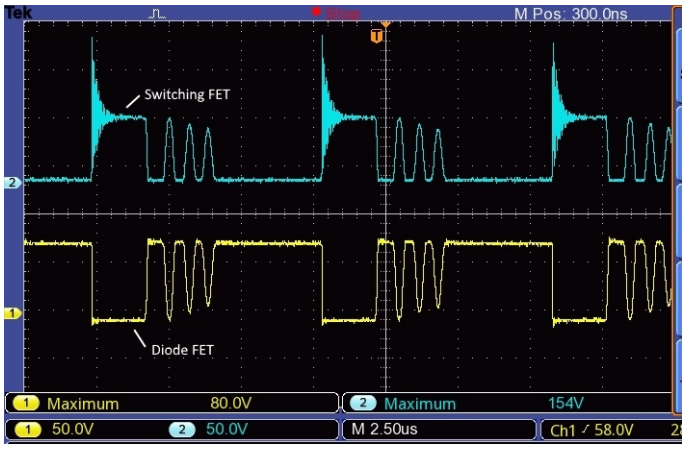

Figure 5-14: Vds over each MOSFET, Vin=48V, Vout=48V

For the sake of component durability we inspected our converter with a thermal camera. The image can be seen in figure 5-15, with the corresponding electrical conditions. Evident are 3 hot spots, which coincide with the MOSFETs and the transformer (figure 5-1). The energy flow was from right to left, so it is the switching MOSFET that is getting considerably warm. The heat generated is directly proportional to the efficiency of the converter, so the temperature of the MOSFET would ideally be lower, but is not disastrous for the converter as the MOSFET has a rated operating temperature of 175°C.

Figure 5-15: Thermal image, Vin=24V, Vout=24V, I=1A

Efficiency The efficiency of the converter has not been stated as a requirement or wish and the design has therefore not been centered around efficiency. However, the efficiency of a converter is of interest to the circuit design and pcb layout subsystems as it provides feedback on the effectiveness of the components, the placing of the components and traces, and yields some insight into the operating environments and applications the converter will be suitable for. A rough estimation of the efficiency of our converter under different electrical circumstances can be found in figures 5-16 and 5-17. Note that the efficiency does not exceed 80%, which can be seen as a fairly standard efficiency for non-optimized flyback converters [32].

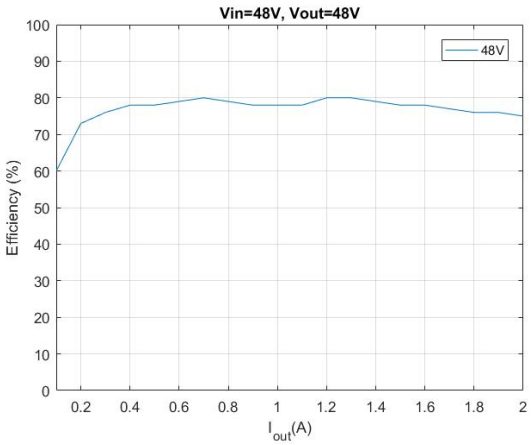

Figure 5-16: Converter efficiency vs. output current, Vin=48V

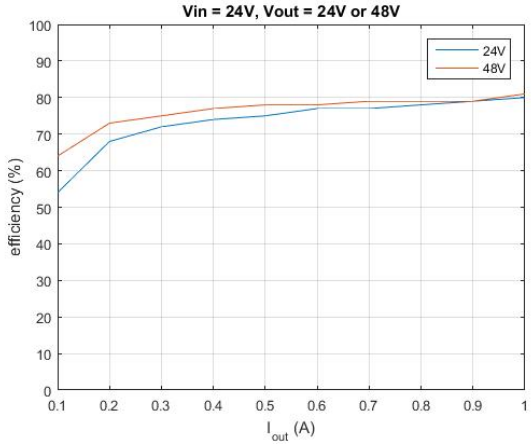

Figure 5-17: Converter efficiency vs. output current, Vin=24V

5.4 Assessment

Overall the design works fairly decent. Some requirements have been achieved, yet others remain to be met. The accomplishment are the following:

- Working bi-directional flyback SMPS topology.
- Full input and output voltage range of 12V to 48V, controllable by a single PWM signal.
- Fast, analog cycle-to-cycle current limiting.
- SMPS operating at 125kHz.
- Stable voltage measurements of input and output.
- Stable primary side current measurement.
- Maximum power transfer of 96W.

The requirements and wishes that remain to be met:

- Maximum power rating of 110W at Vin=48V, Vout=48V.
- Stable current measurement on the secondary side.
- High Efficiency
- General robustness and reliability.

The current prototype works with any input and output ranging from 12V to 48V. However, the power output is still limited due to the power transfer saturation, and is not constant over the entire voltage range. The maximum power output lies at 96W with 48V input and output, with an efficiency of 75%. This is fairly close to the 110W target, but the efficiency is not as high as expected. As for the measurements supplied to the microcontroller, all but the secondary side current measurements work. Due to the flyback topology, it is possible to reflect the primary side measurements to the output by factoring in the non-ideal transformer and the circuit losses.

As for the high temperature produced by the MOSFET, it is not a major problem since the MOSFET can handle this, but for overall system efficiency, reliability and robustness it might be considered to add heat-sinks to the prototype. As for the general prototype robustness, the AUIRFR4620 MOSFET holds up to the high reflected voltages really well, but could be further protected by adding the proposed clamp circuit design.

The power rating requirement has not been met. The causes discussed in section 5.3 are attributed to prototype design, but some mistakes could have been made in an earlier step of macro-circuit design or transformer design.

The secondary-side current measurement failed to work. After inspection it was discovered that because of the current direction in the secondary shunt, the voltage potential of the current measurement is negative with respect to ground. Since our op-amp measurement implementation does not support negative voltages, the measurements are non-existent.

5.5 Next steps

Considering what has been achieved up to this point, there is still more work to be done before this converter can be considered as a viable option for the solar-powered eBike charging station.

Fulfill remaining requirements The most important requirement to fulfill is to reach the power rating of 110W. A possible solution to this, while not completely fixing the problem, is to lower the switching frequency. This increases the maximum power transfer of the converter. The negative side is that this is realized by increasing the peak currents in the transformer, thus producing more electrical stress to the circuit.

Secondly, it is of importance to check what is affecting the efficiency and robustness. By taking the generated heat and location into account, the source of the power loss can be detected. Using a more efficient MOSFET or transformer design might resolve this problem. Robustness, can be improved by applying the designed clamp circuit to the prototype and studying if this might improve the high temperatures measured at the MOSFET.

As for the current measurement on the secondary side, to solve this problem a method would have to be found with which the measurement bridge is also capable of measuring the negative voltages of the secondary shunt, and consequentially producing a usable current measurement.

Prototype improvements There are surely four points where the current prototype PCB can be improved; the ground-plane, footprints/components, heat dissipation and electrical connections. For the ground-plane, make sure that it is included in the prototype seeing that a good ground connection has a big influence on the noise reduction, IC stability and overall system functioning. Furthermore, it is important to make sure the footprints on the PCB are all correct and easy to perform tests on. Some of our footprints were designed wrong, making the soldering and testing more difficult than it could be.
Some traces on the prototype were connected falsely on the PCB design. This can of course always occur when designing the first prototype of a PCB, but these must be noticed and dealt with accordingly. Lastly, making the MOSFET on the PCB compatible with a heatsink would be ideal for optimizing the system in further stages.

Manufacturing considerations Although it is essential to first get the design completely working, for further production of this converter the following might be essential in making the design manufacturing ready.

- The PCB size, and simultaneously the manufacturing price can be reduced by replacing all of the components by their surface-mount device (SMD) variant. This not only decreases size, but also positively influences the functioning of the converter by optimizing critical current paths.

- A housing should be designed, together with standardized connectors if the converter is to be used in the field.

- If the converter is to be brought on the market, EMI tests have to be passed. This involves a critical rethinking of the EMI reduction on the PCB.

Bibliography

[1] Sergio Saponara, Luca Fanucci, Edoardo Biagi and Riccardo Serventi *Hard macrocells for DC/DC converter in automotive embedded mechatronic systems*, EURASIP Journal on Embedded Systems, 2016

[2] TU Delft Campus Green Village, http://www.sustainability.tudelft.nl/projects/campus/

[3] Mr.S.Dhanasekaran, Mr.E.Sowdesh Kumar and Mr.R.Vijaybalaji, *Multiple Output SMPS with Improved Input Power Quality*, Department of Electrical Engineering, Indian Institute of Technology, Delhi,2010

[4] G. M. Ponzo, G. Capponi, P. Scalia and V. Boscaino, *An Improved Flyback Converter*, University of Palermo, May 2009

[5] Jean Picard, *Under the hood of flyback SMPS design* Texas Instruments Power Supply Design Seminar, 2010

[6] J. Formenti and R. Martinez, *Design Trade-offs for Switch-Mode Battery Charger*, Texas Instrument, 2004, pg. 1-2.

[7] Transformer datasheet EPCOS, https://en.tdk.eu/inf/80/db/fer_07/etd_29_16_10.pdf

[8] Colonel Wm. T. McLyman, *Transformer and Inductor Design Handbook, 3rd ed.*, Marcel Dekker, Inc, 2004.

[9] Dr.-Ing. Arthur Seibt, Vienna, *The Flyback DC-DC Converter*, Bodo's Power Systems, October 2016, pg. 62-69.

[10] Dr.-Ing. Arthur Seibt, Vienna, *The Flyback DC-DC Converter*, Bodo's Power Systems, November 2016, pg. 70-83.

[11] Henry J. Zhang, *PCB Layout Considerations for Non-Isolated Switching Power Supplies*, Application note 136, Linear Technology, June 2012

[12] Sameer Kelkar, *The Fundamentals of Flyback Power Supply Design*, Power Integrations, Inc. (San Jose, CA) , 2012.

[13] Wikipedia, the free encyclopedia https://en.wikipedia.org/wiki/Proximity_effect_(electromagnetism)

[14] Infineon Technologies, *Automotive MOSFETs: Prouct Overview*, 2016

[15] Hangseok Choi, Ph. D, *Practical Feedback Loop Design Considerations for Switched Mode Power Supplies*, Fairchild Semiconductor Power Seminar, 2010 - 2011.

[16] H. Dean Venable, *The K Factor: A new mathematical tool for stability analysis and synthesis*, Venable Industries, Inc, 1983.

[17] *Introduction to SMPS Control Techniques*, Microchip Technology, inc., WebSeminar, 2006.

[18] Loyd Dixon, *Designing planar magnetics*, Texas Instruments.

[19] Delta, TU Delft,http://www.ridleyengineering.com/design-center-ridley-engineering.html

[20] Loyd H. Dixon, Jr *Eddy Current Losses in Transformer Windings and Circuit Wiring*, Texas Instruments, 2003.

[21] Gwan-Bon Koo/ Ph. D *Application Note AN-4147: Design Guidelines for RCD Snubber of Flyback Converters*, Fairchild Semiconductor, 2006.

[22] Ashraf A. Mohammed and Samah M. Nafie *Flyback Converter Design for Low Power Application*, Sudenese Electricity Distribution Company.

[23] Andrew Smith *Calculating power loss in switching MOSFETs*, Power Integrations, Inc., 2011.

[24] Toshiba Corporation. *Power MOSFET: Selecting MOSFETs and Consideration for Circuit Desing*, 2016.

[25] Gurkan Tosun, Omer Cihan Kivanc, Ender Oguz, Ozgur Ustun, and R. Nejat Tuncay *Development of High Efficiency Multi-Output Flyback Converter for Industrial Applications*

[26] VOLTECHNOTES *Measuring Leakage Inductance*, Voltech Instruments Ltd., 2001.

[27] Hector Ortega Jimenez *AC resistance evaluation of foil, round and Litz conductors*, Chalmer's university of technology, 2013.

[28] Henry J. Zhang, *PCB Layout Considerations for Non-Isolated Switching Power Supplies*, Linear Technology, Application note 136, June 2012.

[29] Infineon Technologies, *HEXFET power MOSFETs, AUIRFR4620 datasheet*, May 2015.

[30] Texas Instruments, *Current Mode PWM Controller, UC2845N datasheet*, May 2002.

[31] Texas Instruments, *Switching Voltage Regulators, LM2575HV datasheet*, April 2013.

[32] Brian Huffman, *Efficiency and Power Characteristics of Switching Regulator Circuits*, Linear Technology, Application note 46, November 1991.

[33] Ken Kundert, *Power Supply Noise Reduction*, The Designer's Guide Community, Version 4, January 2004.

[34] Adrian Nastase, https://masteringelectronicsdesign.com/how-to-derive-the-rms-value-of-a-triangle-waveform/.

[35] BAP group B1, *Control Network of Bi-Directional DC/DC Converters*, TU Delft, June 2017.

Appendix

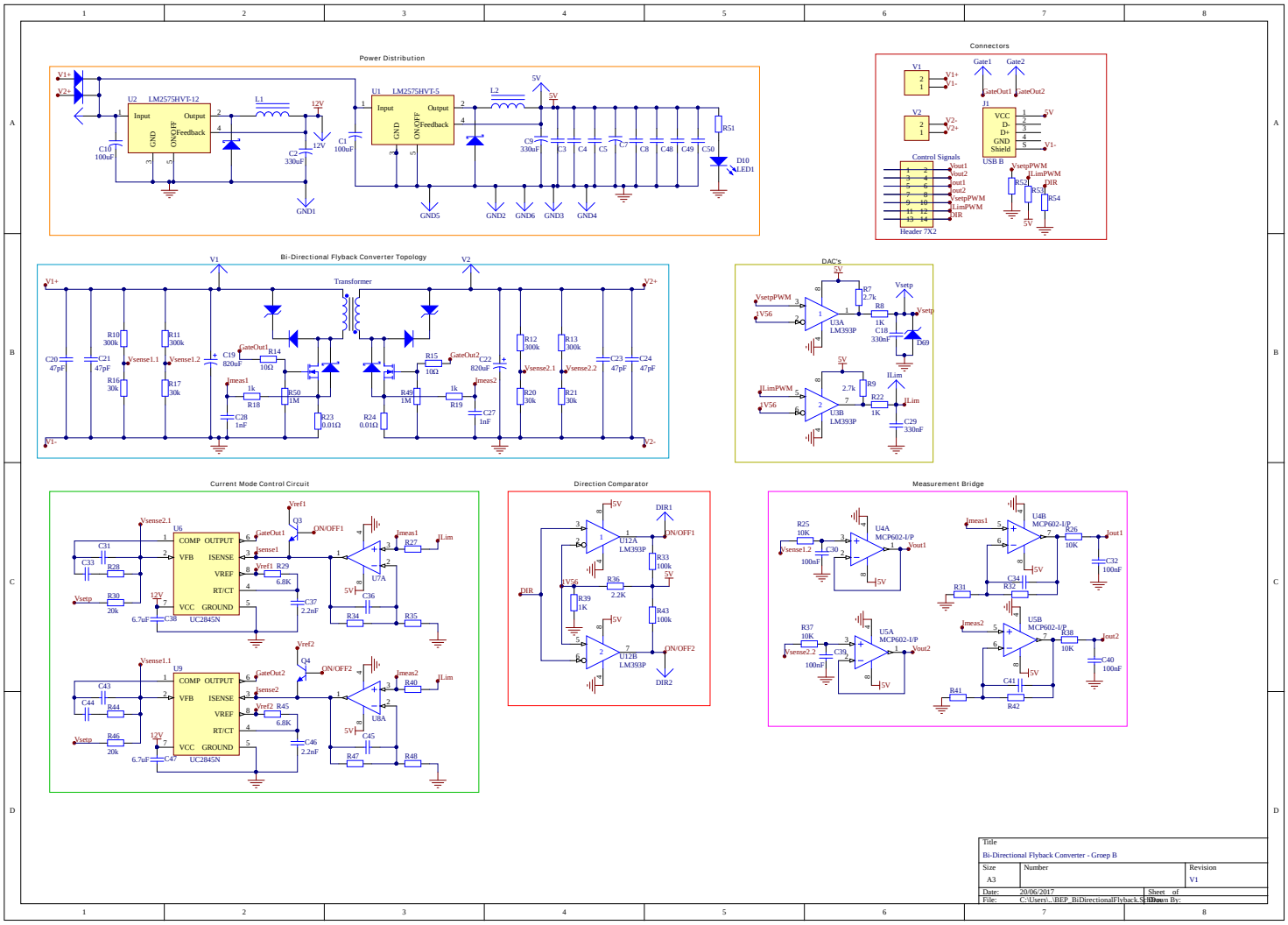

Figure A-1: Altium schematic of the bi-directional flyback converter

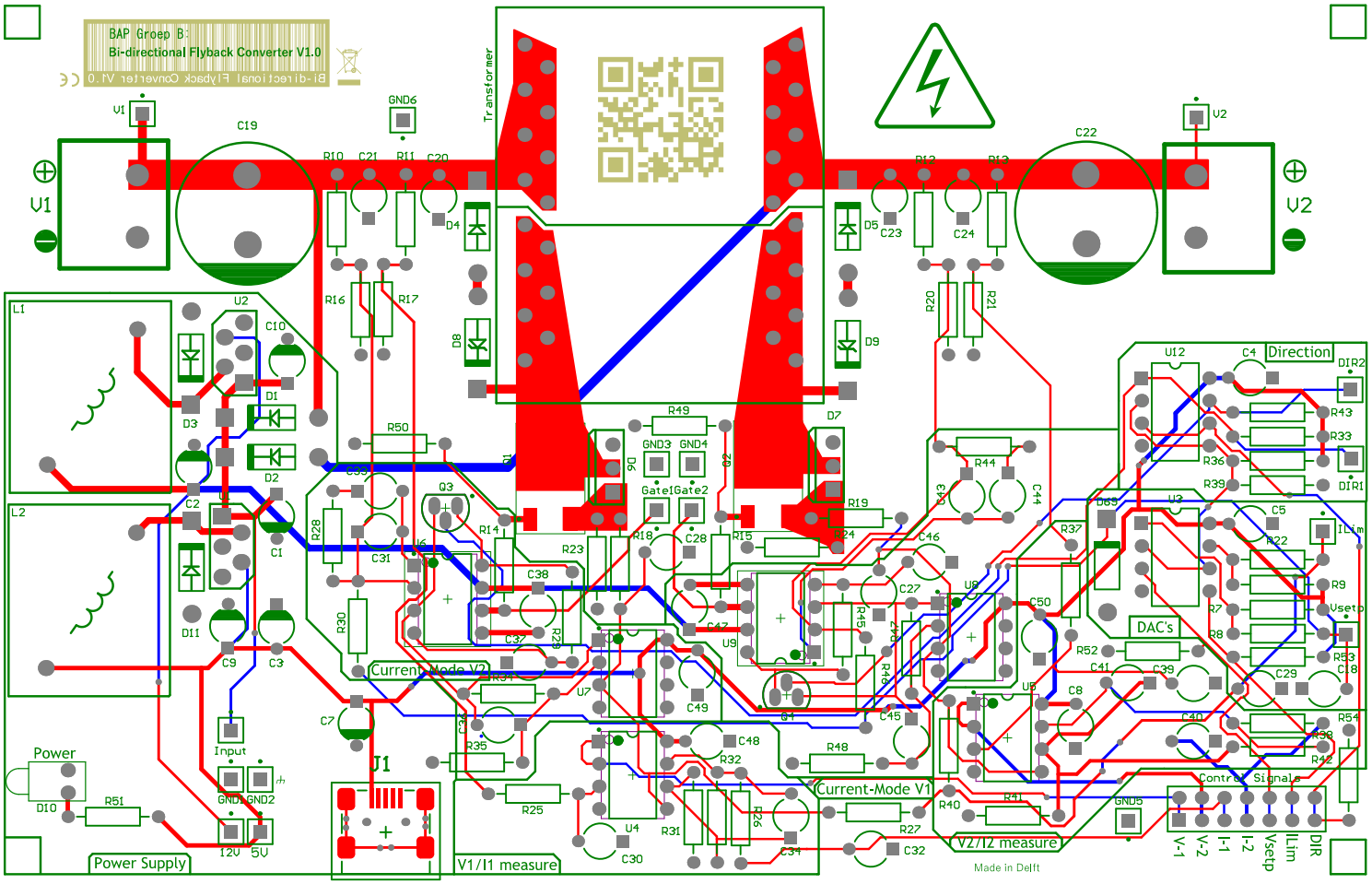

Figure A-2: Altium PCB of the bi-directional flyback converter

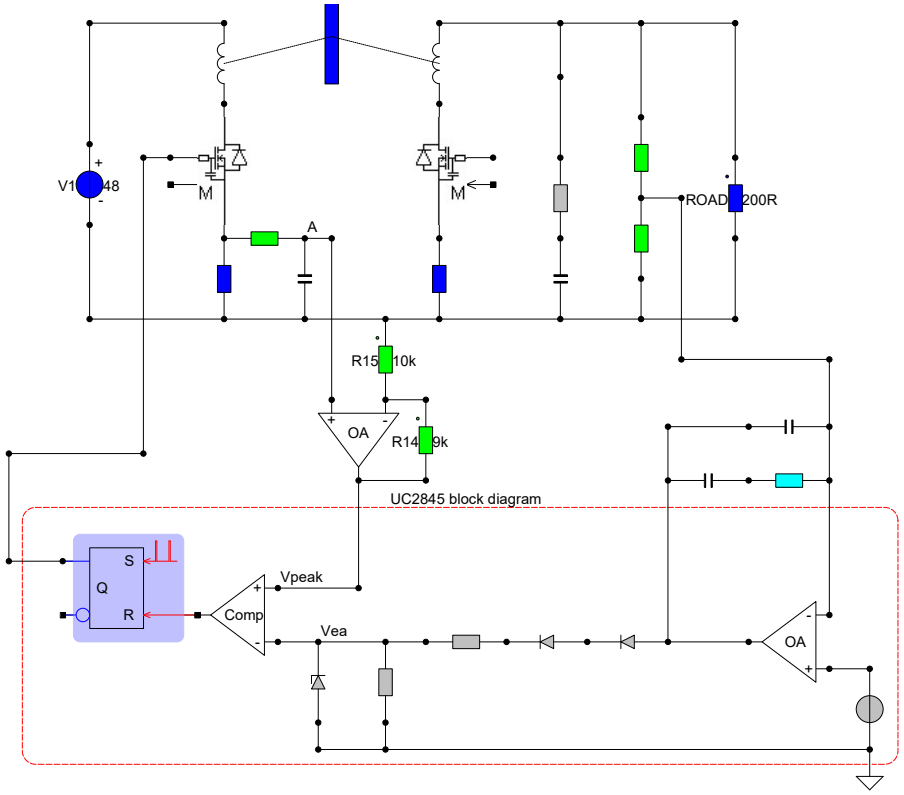

Figure A-3: Block diagram implementation of the UC2845 internal control loop

Figure A-4: Measurement of primary inductance at 125KHz $L1 = 19,49\mu H$ and $R1 = 340,69m\Omega$

Figure A-5: Measurement of secondary inductance at 125KHz $L2 = 19,77\mu H$ and $R2 = 402,35m\Omega$

Errata

1. From the appendix, figures A-4 and A-5 have been corrected to figures A-6 and A-7.

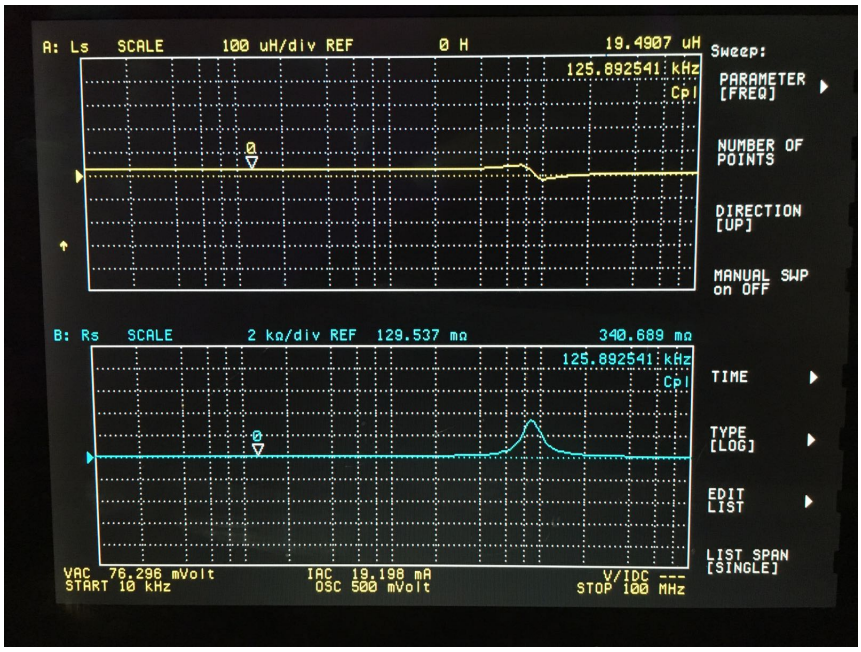

Figure A-6: Copper, ⌀1.25mm, primary inductance, @125KHz, $L1 = 19,49\mu H$ and $R1 = 340,69m\Omega$

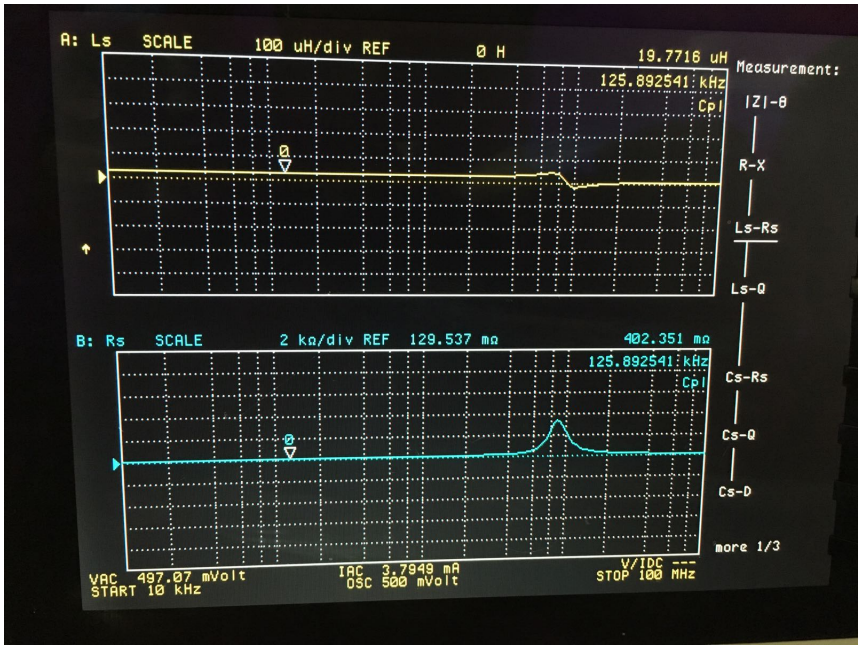

Figure A-7: Copper, ⌀1.25mm, secondary inductance, @125KHz, $L2 = 19,77\mu H$ and $R2 = 402,35m\Omega$

2. The formulas stated in section 2.2.1 are based on the paper from Seibt[9], [10]. Furthermore, In section 2.2.1, an initial estimation is made regarding the resistance of the wire. However, there is another factor that could be calculated which is the resistance of the core itself. The resistance of the core is a constant based on the dimensions of the core and the gap. The following formula is valid,

$$R_m = \frac{\frac{l_e}{\mu_r} + l_g}{\mu_o \cdot A_e} \tag{A-1}$$

with,

- Rm, resistance of the core
- e, effective length of the core
- μ_r, permeability of the core
- lg, effective length of the air gap
- μ_o, permeability in free space